Supporting Information

Polymer-Supported-Cobalt-Catalyzed Regioselective Cyclotrimerization of Aryl Alkynes

Abhijit Sen, Takuma Sato, Aya Ohno, Heeyoel Baek, Atsuya Muranaka, Yoichi M. A. Yamada*

RIKEN Center for Sustainable Resource Science, Wako, Saitama 351-0198, Japan

E-mail: ymayamada@riken.jp

Contents

1. General

All chemicals and solvents were used as received without further purification unless otherwise mentioned. ^{1}H-NMR (500 MHz), ^{13}C-NMR (125 MHz), and ^{19}F-NMR (470 MHz) spectra were measured with a JEOL JNM ECA-500 spectrometer at 25 °C. Chemical shifts (δ) are expressed relative to the resonances of the residual non-deuterated solvent for ^{1}H [$CDCl_3$: ^{1}H (δ) = 7.26 ppm, acetone-d_6: ^{1}H (δ) = 2.05 ppm], ^{13}C [$CDCl_3$: ^{13}C (δ) = 78.0 ppm, acetone-d_6: ^{13}C = 29.8 and 206.3 ppm]. Absolute values of the coupling constants are given in Hertz (Hz), regardless of their sign. Multiplicities are abbreviated as singlet (s), doublet (d), doublet of doublets (dd), triplet (t), quartet (q), quintet (quint), multiplet (m), and broad (br). Inductively coupled plasma mass spectrometry (ICP-MS) measurement was performed on a Perkin Elmer Nexion 300D. All the chemicals were purchased from commercial sources and used as received. Cyclotrimerization reactions were carried out using an organic synthesizer, ChemiStation (EYELA, PPS-1511). TLC analysis was performed on Merck silica gel 60 F254. Flash column chromatography was carried out using Wakogel silica C-200 (particle size: 75-150 μm). A series of combinations of ethyl acetate and hexane was used as an eluent. The Matrix-Assisted Laser Desorption/Ionization-Time of Flight (MALDI-TOF) mass spectroscopy (MS) was measured by using 2,5-dihydroxybenzoic acid as matrix in a Bruker rapifleX MALDI Tissuetyper on Positive mode and Reflector mode. X-ray photoelectron spectroscopy (XPS) experiments of catalyst and recovered catalyst were performed with AXIS-NOVA (Kratos) using Monochromatic Al Kα 150W (15kV×10mA) excitation source at Saitama University. The recovered catalyst sample was treated in a glovebox filled with argon and transferred to the analysis chamber without air-exposure using a transfer vessel. The Gas Chromatography Mass Spectrometry (GC-MS) was measured by using Agilent Technologies 7890B equipped with a HP-1 capillary column. SEM images were obtained by using a Thermoscientific QuattroS and the EDX images were obtained by using a Hitachi TS3030Plus/Bruker nanoGmbH Quantax 70

The starting materials **1q**[1], **1k**[2], **1l**[3], **1m**[4], **1n**[5], **1o**[6], **1p**[7], **L6**[8] and **L7**[8] were prepared following the literature report.
XAFS experiment of Co K-edge (7.71 keV) was performed at BL14B2, SPring-8 (JASRI), Japan. All the spectra were measured at room temperature using Si (111) monochromator and ion chambers in transmission mode. The data processing was performed using Demeter software package[9] and FEFF6 code[10]. Density functional theory (DFT) calculation was carried out using ORCA program package.[11] BP86 functional and Grimme's D3BJ dispersion correction[12] with def2-TZVP basis set was used for the calculation.

2.1. Preparation of poly(4-vinylpyridine) Supported Cobalt Catalyst (P4VP-$CoCl_2$)

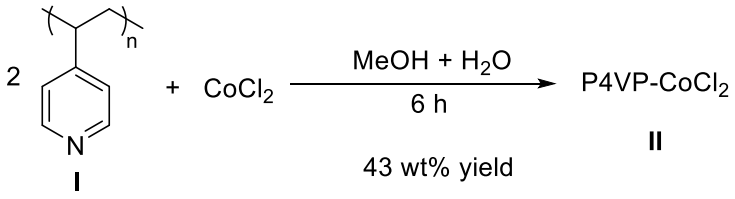

Procedure: Poly(4-vinylpyridine), P4VP (average M_w = 160000, Aldrich, 210 mg) was dissolved in 10 mL of methanol. An aqueous solution (10 mL) of $CoCl_2$ (130 mg) was slowly added to the polymer containing methanol solution. A precipitate was observed during slow addition. The reaction mixture was stirred for more 6 h at room temperature. After that, the precipitate was filtered and the filtrate was discarded. The residue was washed with water (3x10 mL), methanol

(4x10 mL) and diethyl ether (5x5 mL). Next, the residue was collected and dried over vacuum for overnight (15 h) to get polymer supported cobalt complex P4VP-$CoCl_2$ **II** (blue) with 43 wt% yield (147 mg).

2.2. XAFS Analysis

The coordination structure of P4VP-Co was investigated by X-ray absorption fine structure (XAFS) at Co K-edge. Comparing X-ray absorption near edge structure (XANES) of P4VP-$CoCl_2$ with that of known materials (Co foil, Co(II)O, Co(II)$Cl_2{\cdot}6H_2O$, and Co_3(II, III)O_4), it shows similar features to the Co(II) compounds in terms of the position of absorption edge energy and white line (Figure S1a). Although elemental analysis of P4VP-Co indicated that the molar ratio of Co:Cl:N was ca. 1:2:9, Fourier transform of extended X-ray absorption fine structure (EXAFS) implies the lack of Co-Cl bond besides Co-N bond (Figure S1b). Therefore, we proposed an ion pair model as a local structure in P4VP-$CoCl_2$, in which the Co(II) center is positively charged (2+) and it is neutralized by two chloride ions (Cl^-) located outside the coordination sphere (Figure S1c). Next, the optimized geometry of $[Co(4\text{-methylpyridine})_4]^{2+}$ was successfully obtained as a tetrahedral dicationic complex in high-spin state based on density functional theory (DFT) at the level of BP86-D3BJ/def2-TZVP (Figure S1d). After all, the fitting on the first coordination shell of the experimental data with the DFT-based model shows an acceptable result with Co-N bond length of 2.140 Å and R factor of 0.024 (Figures S1b and S2).

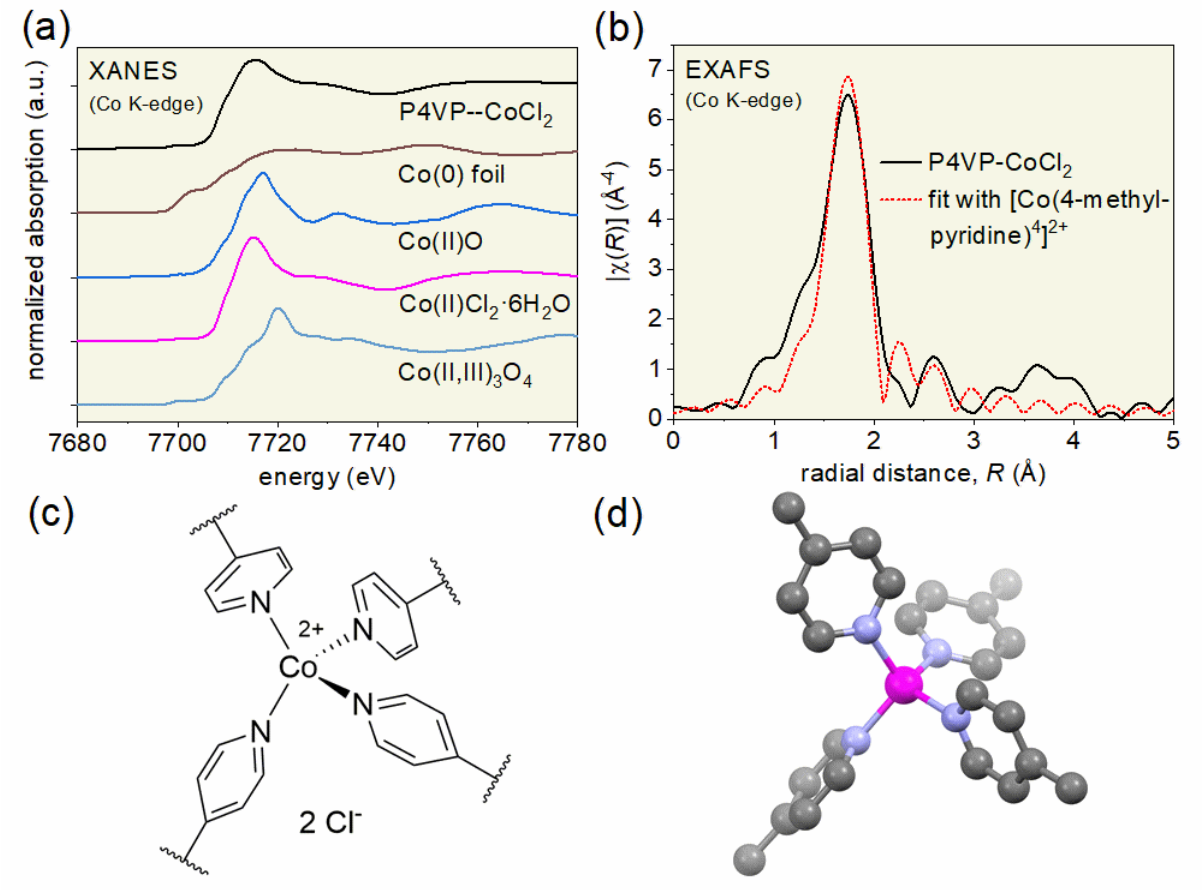

Figure S1. (a) Co K-edge XANES; (b) radial distribution function (RDF) of P_4VP-$CoCl_2$ and the best fit (k-range: 3-12 $Å^{-1}$, R-range: 1.2-2.1 Å, R(Co-N) = 2.140(16) Å, σ^2 = 0.0041(10) $Å^2$, R factor = 0.024); (c) proposed local structure of P4VP-$CoCl_2$ as an ion pair; (d) DFT-optimized structure of $[Co(4\text{-methylpyridine})_4]^{2+}$ (BP86-D3BJ/def2-TZVP). Hydrogen atoms are omitted for clarity.

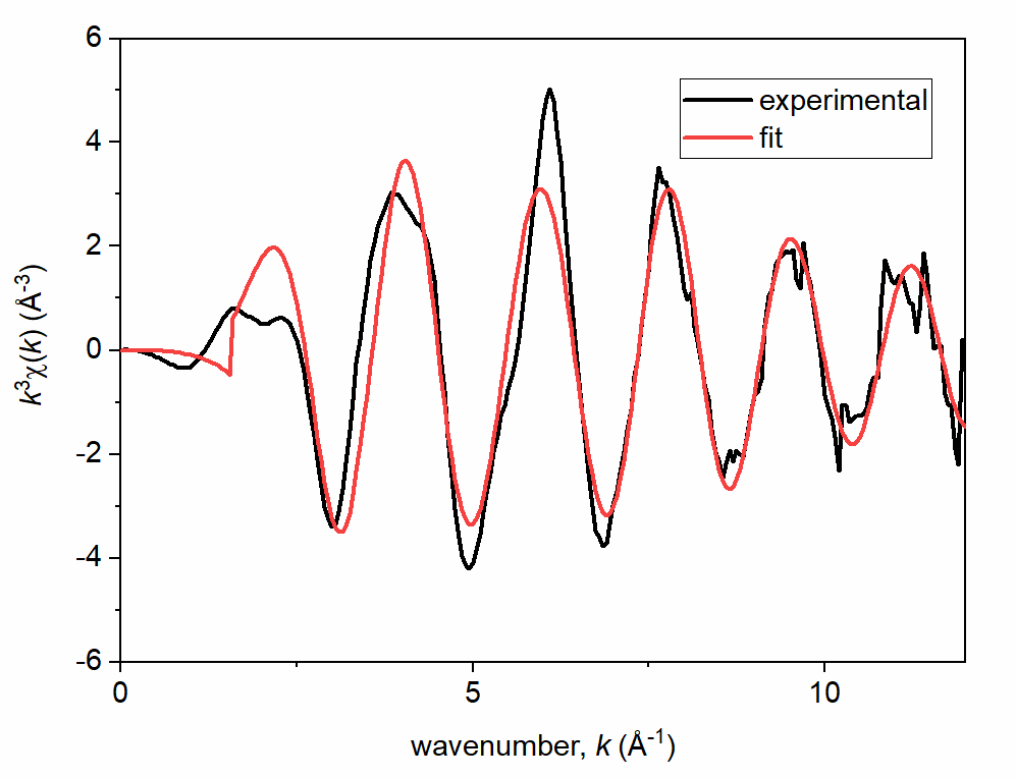

Figure S2. k^3-Weighted EXAFS (Co K-edge) of P4VP-$CoCl_2$ and the best fit with high-spin $[Co(4\text{-methylpyridine})_4]^{2+}$.

2.3. Optimized Cartesian Coordinates of High-Spin $[Co(4\text{-methylpyridine})_4]^{2+}$ (BP86-D3BJ/def2-TZVP).

Co	-0.00175755293238	-0.00194419527156	0.15244879394296
N	-1.66510410737387	0.06180339106212	-0.93814113957131
N	1.61238092212944	-0.03125360069533	-1.01113937103629
N	-0.02050676663784	1.61974924086406	1.30574382868980
N	0.06547520865357	-1.65800691189360	1.25377013877378
C	0.33215458845825	1.57061398018728	2.61222651123748
C	-1.03667748135893	-2.41215372264319	1.47672022655396
C	0.33853097542403	2.69594567611980	3.42250393893807
C	-1.00664676044286	-3.55902330333911	2.25598260811509
C	-0.02705757443415	3.94753413725090	2.89941238910805
C	0.19422978477213	-3.97973850370378	2.85100806598246
C	-0.39605102940360	3.98115714720457	1.54258536348813
C	1.33141236406685	-3.18892413220987	2.60541275337648
C	-0.38302666188794	2.81938541885598	0.78778375359429
C	1.23430839272529	-2.05503997298341	1.81548010027805
C	-0.00759607060595	5.18613468154529	3.73699254913499
C	0.25998674730532	-5.19681081454084	3.71732114515522

H	0.60585337733664	0.59079996461149	3.00480678824806
H	-1.95910438601561	-2.07635247050712	1.00189108572593
H	0.62562512554760	2.59518975133733	4.46946194402718
H	-1.92446232275627	-4.13058836183164	2.39586696551175
H	-0.70086512222371	4.91708327011874	1.07352058102912
H	2.29893239793540	-3.46197332606490	3.02767165259984
H	-0.67650251812236	2.82563353474584	-0.26339425404479
H	2.10838529128335	-1.43586708737104	1.60636108912579
H	-0.15339920544552	4.95910007150900	4.80010416531452
H	1.22411188498625	-5.71151400548974	3.61611021980646
H	-0.77057652307431	5.90508301858523	3.41296729100623
H	-0.55020553929235	-5.90050886622195	3.49181354743294
H	0.97092073285056	5.68499804057462	3.63939335228329
H	0.15928763085641	-4.90542459741278	4.77594715504035
C	3.87317429090609	-0.10498294238360	-2.69684786177589
C	3.47651031494428	1.07499506305872	-2.04504828720379
C	2.35962296883009	1.07815175070644	-1.22352873681545
C	1.98644626385261	-1.17955022162917	-1.62735683008487
C	3.09046447476854	-1.24938735255156	-2.46191686114274
C	5.05740340306697	-0.13774101580649	-3.60934009198763
H	4.04393819323298	1.99706110628706	-2.17383496225704
H	2.04303862793665	1.98343480669511	-0.70458738223681
H	1.37431132617328	-2.06037439817310	-1.42589296699153
H	3.34636829233712	-2.20160869882222	-2.92732912117091
C	-4.05042559633934	0.12979800128296	-2.44276623917138
C	-4.03211353580335	0.45175672001407	-1.07399451273259
C	-2.84299998026872	0.40949195880406	-0.36376569076490
C	-1.66592549579969	-0.24575426934028	-2.25710788133319
C	-2.82039385977420	-0.22102624318729	-3.02453128686339
C	-5.31858577583588	0.14200559870238	-3.23503493200517
H	-4.94872737926625	0.74282937719576	-0.56026255745745
H	-2.80916432485793	0.66633835195459	0.69643534833068
H	-0.70244787459496	-0.50856433728975	-2.69493812073536
H	-2.75967513630026	-0.47203299171338	-4.08381050764148
H	-5.78442196723230	-0.85699996125191	-3.20532951503403
H	-5.13411642541822	0.38207783929932	-4.28956389070441
H	-6.04628001619879	0.85278475918081	-2.82447631809999
H	5.51039758069389	-1.13594972868246	-3.65005433069407
H	5.81895906391261	0.59291894201006	-3.30954418970690
H	4.74358676471132	0.12124043324746	-4.63420551258757

2.4. Elemental Analysis:

Co: calculated 5.13%, observed 5.14%; Cl: calculated 6.18%, observed 6.08%; C: calculated 65.90%, observed 65.88%; H: calculated 6.18%, observed 6.12%; N: calculated 10.98%, observed 10.85%.

2.5. Scanning Electron Microscope (SEM) and Energy Dispersive X-Ray Analysis (EDX) Analysis

For getting the SEM images the sample was treated with PdPt alloy sputtering for 30 s before working.

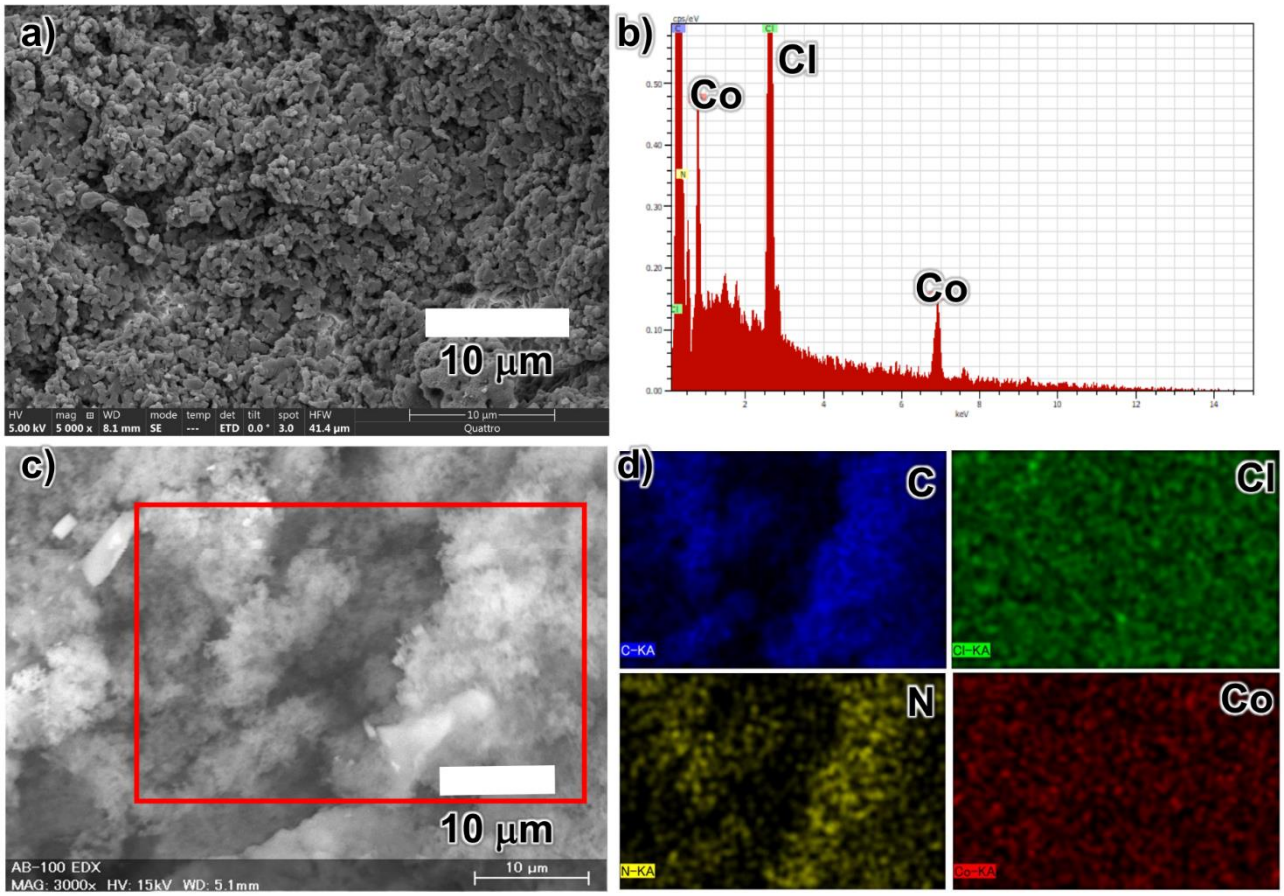

Figure S3. SEM and EDX images of P4VP-$CoCl_2$.

3. Optimization of Reaction Conditions [a]

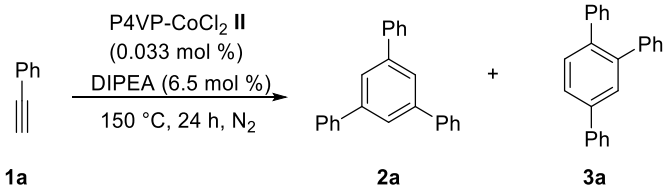

1a **2a** **3a**

entry	deviation from standard conditions	yield of **2a** (%)	yield of **3a** (%)
1	none	69 (68[b])	0
2	without base	64	0

3	1 mol equiv of base	68	0
4	100 °C	trace	0
5	15 h	57	0
6	zinc (1 mol equiv)	63	0
7	zinc (5 mol equiv)	47	0
8	manganese (1 mol equiv)	66	0
9	0.015 mol % P4VP-$CoCl_2$ (150 mol ppm Co)	59	0
10	0.066 mol % P4VP-$CoCl_2$ (660 mol ppm Co)	68	0
11	0.033 mol % P4VP-$CoBr_2$ (330 mol ppm Co)	66	0
12	$CoCl_2$ (0.3 mol % Co) and P4VP (1.3 mol %)	24	6
13	in toluene (0.5 mL)	40	0
14	in xylene (0.5 mL)	66	0
15	in DMF (0.5 mL)	trace	0
16	in the absence of cobalt	0	0
17	air instead of N_2	44	0

[a] The reactions were performed with 1 mol equiv of **1a**, 0.033 mol % of catalyst **II**, 6.5 mol % of DIPEA at 150 °C for 24 h under N_2. The yield was determined by ^{1}H-NMR studies using 1,3,5-trimethoxybenzene as internal standard. [b] isolated yield.

4. Homogeneous Reactions [a]

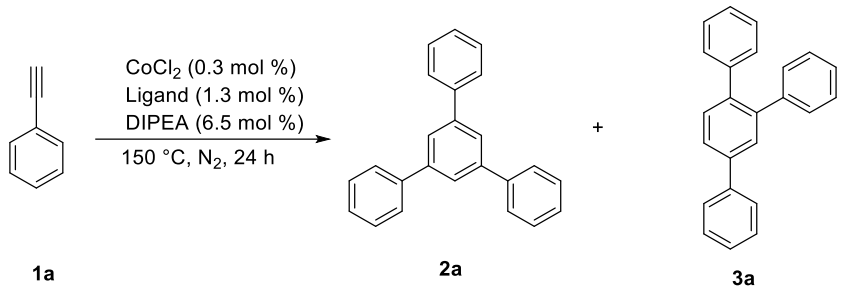

entry	catalyst	ligand	yield of **2a** (%)	yield of **3a** (%)
1	$CoCl_2$	-	trace	9
2	$CoCl_2$	L1	4	7
3	$CoBr_2$	L1	4	3
4	CoI_2	L1	0	0
5	CoF_2	L1	0	1
6[b]	$CoCl_2$	L1	7	12
7	$CpCo(CO)_2$	L1	15	21
8	$(PPh_3)_3CoCl$	L1	1	0
9	$CoCl_2$	L2	16	20

10	$CoCl_2$	L3	19	24
11	$CoCl_2$	L4	4	8
12	$CoCl_2$	L5	5	6
13	$COCl_2$	L6	0	0
14	$CoCl_2$	L7	5	7
15	$CoCl_2$	L8	6	11
16	$CoCl_2$	L9	9	11

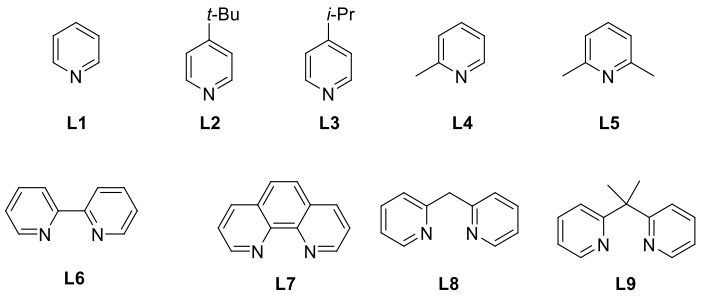

[a] The reactions were performed with 1 mol equiv of **1a**, 0.3 mol % of catalyst, 1.3 mol % of Ligand, 6.5 mol % of DIPEA at 150 °C for 24 h under N_2. The yield was determined by ^{1}H-NMR studies using 1,3,5-trimethoxybenzene as internal standard. [b] Reaction was performed with pre-complexed metal-ligand catalyst.

5. Catalysis

5.1. General Procedure for Cyclotrimerization Reaction

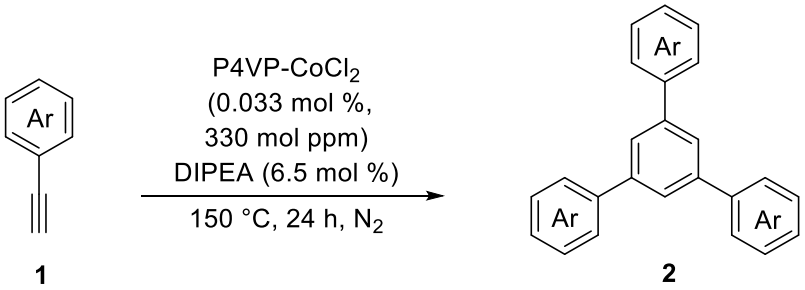

A mixture of P4VP-$CoCl_2$ (330 mol ppm, 1.85 mg), aryl alkyne, **1** (1 mol equiv, 5 mmol), and DIPEA (6.5 mol %, 42 mg) were added to a reaction tube. The reaction tube was degassed under vacuum and refilled with N_2 under standard Schlenk techniques (3 times). The reaction tube was sealed with screw cap and Teflon then placed over a chemiStation (metal block) under nitrogen for 24 h. After the reaction, the reaction mixture was diluted by EtOAc (approximately 5 mL) and filtered through a celite pad, and washed with EtOAc. The EtOAc solution was collected. The solvent was evaporated under vacuum and crude mass was purified by column chromatography to give product **2**. The yield of the isolated product was determined based on a single experiment.

5.2. Characterization of Products

1,3,5-triphenylbenzene (2a, Ref. 13**)**

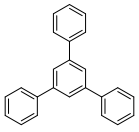

The molecule was purified by column chromatography using hexane as eluent. White solid (68% yield, 345 mg). m. p. 175-176 °C; ^{1}H-NMR (500 MHz, $CDCl_3$) δ 7.79 (s, 3H), 7.71 (d, J = 7.2 Hz, 6H), 7.49 (t,

J = 7.2 Hz, 6H), 7.40 (t, J = 7.2 Hz, 3H). $^{13}C\{^1H\}$-NMR (125 MHz, $CDCl_3$) δ 142.5, 141.3, 129.0, 127.6, 127.5, 125.3.

1,3,5-tris(4-methylphenyl)benzene (2b, Ref. 13**)**

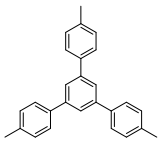

The molecule was purified by column chromatography using hexane as eluent. White solid (84% yield, 485 mg). m. p. 175-176 °C; ^1H-NMR (500 MHz, $CDCl_3$) δ 7.74 (s, 3H), 7.60 (d, J = 8.0 Hz, 6H), 7.29 (d, J = 8.0 Hz, 6H), 2.42 (s, 9H). $^{13}C\{^1H\}$-NMR (125 MHz, $CDCl_3$) δ 142.3, 138.5, 137.4, 129.6, 127.3, 124.7, 21.2.

1,3,5-tris(4-methoxyphenyl)benzene (2e, Ref. 13**)**

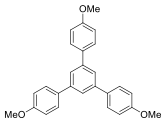

The molecule was purified by column chromatography using hexane as eluent. White solid (86% yield, 567 mg). m. p. 141-142 °C; ^1H-NMR (500 MHz, $CDCl_3$) δ 7.65 (s, 3H), 7.62 (dd, J = 6.6, 2.0 Hz, 6H), 7.01 (dd, J = 6.6, 2.0 Hz, 6H), 3.87 (s, 9H). $^{13}C\{^1H\}$-NMR (125 MHz, $CDCl_3$) δ 159.4, 142.0, 134.4, 128.5, 123.9, 114.3, 55.5.

1,3,5-tris(4-butylphenyl)benzene (2f, ref. 14**)**

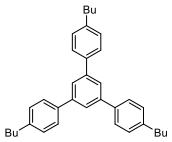

The molecule was purified by column chromatography using hexane as eluent. Colorless liquid (79% yield, 622 mg). ^1H-NMR (500 MHz, $CDCl_3$) δ 7.75 (s, 3H), 7.61 (d, J = 8.0 Hz, 6H), 7.29 (d, J = 8.0 Hz, 6H), 2.68 (t, J = 7.4 Hz, 6H), 1.63-1.69 (m, 6H), 1.41 (td, J = 14.9, 7.4 Hz, 6H), 0.96 (t, J = 7.4 Hz, 9H). $^{13}C\{^1H\}$-NMR (125 MHz, $CDCl_3$) δ 142.4, 142.2, 138.7, 120.0, 127.3, 124.7, 35.4, 33.8, 22.5, 14.1. Elemental analysis calcd (%) for $C_{36}H_{42}$: C 91.08, H 8.92; found: C 91.06, H 8.91.

1,3,5-tris(4-bromophenyl)benzene (2g, Ref. 13**)**

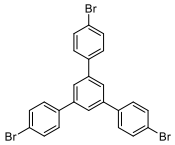

Xylene (0.5 mL) was added as solvent. The molecule was purified by column chromatography using hexane as eluent followed by recrystallization (hexane/ethyl acetate) of the isolated product. Light yellow solid (66%, 591 mg). m. p. 161-162 °C; ^1H-NMR (500 MHz, $CDCl_3$) δ 7.69 (s, 3H), 7.60 (d, J = 8.6 Hz, 6H), 7.53 (d, J = 8.6 Hz, 6H). $^{13}C\{^1H\}$-NMR (125 MHz, $CDCl_3$) δ 141.6, 139.7, 132.1, 129.0, 125.1, 122.2.

1,3,5-tris(4-chlorophenyl)benzene (2h, Ref. 13**)**

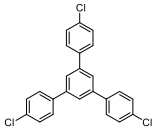

Xylene (0.5 mL) was added as solvent. The molecule was purified by column chromatography using hexane as eluent followed by recrystallization (hexane) of the isolated product. White solid (61%, 414 mg). m. p. 245-246 °C; ^1H-NMR (500 MHz, $CDCl_3$) δ 7.68 (s, 3H), 7.59 (d, J = 8.2 Hz, 6H), 7.45 (d, J = 8.2 Hz, 6H). $^{13}C\{^1H\}$-NMR (125 MHz, $CDCl_3$) δ 141.6, 139.3, 134.0, 129.2, 128.6, 125.1, 77.4, 77.1, 76.9.

1,3,5-tris(4-fluorophenyl)benzene (2i, Ref. 13**)**

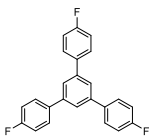

The molecule was purified by column chromatography using hexane as eluent. White solid (53%, 191 mg). m. p. 238-239 °C; ^1H-NMR (500 MHz, $CDCl_3$) δ 7.66 (s, 3H), 7.62-7.65 (m, 6H), 7.15-7.18 (m, 6H). $^{13}C\{^1H\}$-NMR (125 MHz, $CDCl_3$) δ 163.8 (d, J_F = 245.6 Hz), 141.6, 137.1 (d, J_F = 3.4), 129.0 (d, J_F = 8.4), 124.9, 115.8 (d, J_F = 21.5 Hz). ^{19}F-NMR (470 MHz, $CDCl_3$) δ -114.91.

1,3,5-tris(4-(trifluoromethyl)phenyl)benzene (2j, Ref. 13**)**

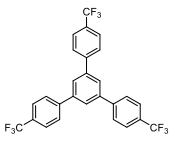

The molecule was purified by column chromatography using hexane as eluent followed by preparative thin layered chromatography (PTLC). White solid (42%, 214 mg). m. p. 232-234 °C; ^1H-NMR (500 MHz, $CDCl_3$) δ 7.81-7.75 (m, 15H). $^{13}C\{^1H\}$-NMR (125 MHz, $CDCl_3$) δ 144.2, 141.8, 130.3 (q, J_F = 32.4 Hz), 127.9, 126.4, 126.3 (q, J_F = 3.5 Hz), 124.5 (q, J_F = 270.0 Hz). ^{19}F-NMR (470 MHz, $CDCl_3$) δ -62.35.

1,3,5-tris(4-(phenyl)phenyl)benzene (2n, Ref. 15**)**

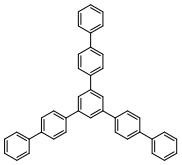

Xylene (0.5 mL) was added as solvent. The molecule was purified by column chromatography using hexane/dichloromethane (19:1) as eluent. White solid (49%, 433 mg). m. p. 230-232 °C; ^{1}H-NMR (500 MHz, $CDCl_3$) δ 7.89 (s, 3H), 7.81 (d, *J* = 8.4 Hz, 6H), 7.74 (d, *J* = 8.4 Hz, 6H), 7.65-7.68 (m, 6H), 7.48 (t, *J* = 7.4 Hz, 6H), 7.38 (t, *J* = 7.4 Hz, 3H). ^{13}C{^{1}H}-NMR (125 MHz, $CDCl_3$) δ 142.1, 140.7, 140.5, 140.1, 128.9, 127.8, 127.7, 127.5, 127.2, 125.1.

1,3,5-tris(4-hydroxyphenyl)benzene (2m, Ref. 16**)**

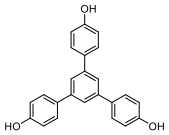

Xylene (0.5 mL) was added as solvent. The molecule was purified by column chromatography using hexane/ethanol (5:1) as eluent. White solid (71%, 417 mg). m. p. 231-233 °C; ^{1}H-NMR (500 MHz, Methanol-d_3) δ 7.57 (s, 3H), 7.53 (dd, *J* = 9.2, 2.6 Hz, 6H), 6.87 (dd, *J* = 9.2, 2.6 Hz, 6H). ^{13}C{^{1}H}-NMR (125 MHz, Methanol-d_3) δ 157.0, 142.0, 132.8, 127.9, 122.6, 115.3.

1,3,5-tris(3-methylphenyl)benzene (2c, Ref. 17**)**

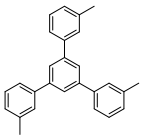

The molecule was purified by column chromatography using hexane as eluent. White solid (77%, 445 mg). m.p. 116-117 °C; ^{1}H-NMR (500 MHz, $CDCl_3$) δ 7.76 (s, 3H), 7.50 (d, *J* = 8.0 Hz, 6H), 7.37 (t, *J* = 7.8 Hz, 3H), 7.21 (d, *J* = 7.8 Hz, 3H), 2.45 (s, 9H). ^{13}C{^{1}H}-NMR (125 MHz, $CDCl_3$) δ 142.5, 141.3, 138.5, 128.8, 128.3, 128.3, 125.2, 124.6, 21.7.

1,3,5-tris(2-methylphenyl)benzene (2d, Ref. 17**)**

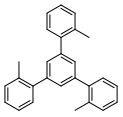

The molecule was purified by column chromatography using hexane as eluent. White solid (67%, 387 mg). m.p. 138-139 °C; ^{1}H-NMR (500 MHz, $CDCl_3$) δ 7.29-7.37 (m, 15H), 2.42 (s, 9H). ^{13}C{^{1}H}-NMR (125 MHz, $CDCl_3$) δ 141.8, 141.6, 135.5, 130.5, 130.1, 128.7, 127.5, 126.0, 20.8.

1,3,5-tris([1,1'-biphenyl]-2-yl)benzene (2o, Ref. 18**)**

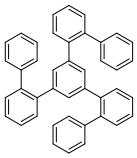

Xylene (0.5 mL) was added as solvent. The molecule was purified by column chromatography using hexane as eluent followed by recrystallization (hexane/ethyl acetate) of the isolated product. White solid (42%, 372 mg). m. p. 215-216 °C; ^{1}H-NMR (500 MHz, $CDCl_3$) δ 7.25-7.38 (m, 18H), 7.05 (dd, *J* = 6.9, 1.7 Hz, 6H), 6.84 (d, *J* = 1.1 Hz, 3H), 6.75 (s, 3H). ^{13}C{^{1}H}-NMR (125 MHz, $CDCl_3$) δ 141.7, 140.8, 140.6, 140.5, 130.6, 130.3, 130.3, 129.9, 128.0, 127.4, 127.3, 126.5.

1,3,5-tris(4-(ethan-1-one)phenyl)benzene (2l, Ref. 15**)**

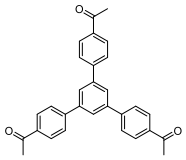

Xylene (0.5 mL) was added as solvent. The molecule was purified by column chromatography using hexane/ethyl acetate (10:1) as eluent followed by recrystallization (hexane/ethyl acetate) of the isolated product. White solid (39%, 280 mg). m. p. 251-252 °C; ^{1}H-NMR (500 MHz, $CDCl_3$) δ 8.09 (d, *J* = 8.6 Hz, 6H), 7.87 (s, 3H), 7.79 (d, *J* = 8.6 Hz, 6H), 2.66 (s, 9H). ^{13}C{^{1}H}-NMR (125 MHz, $CDCl_3$) δ 197.7, 145.1, 141.7, 136.5, 129.2, 127.6, 126.2, 26.8.

1,3,5-tris(4-(ethoxycarbonyl)phenyl)benzene (2k, Ref. 15**)**

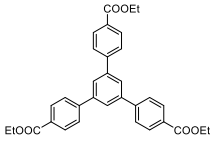

The molecule was purified by column chromatography using hexane/ethyl acetate (19:1) as eluent followed by recrystallization (hexane/ethyl acetate) of the isolated product. White solid (46%, 398 mg). m. p. 180-181 °C; ^{1}H-NMR (500 MHz, $CDCl_3$) δ 8.16 (d, *J* = 8.4 Hz, 6H), 7.85 (s, 3H), 7.76 (d, *J* = 8.4 Hz, 6H), 4.42 (q, *J* = 7.2 Hz, 6H), 1.43 (t, *J* = 7.2 Hz, 9H). ^{13}C{^{1}H}-NMR (125 MHz, $CDCl_3$) δ 166.5, 145.0, 141.8, 130.3, 129.9, 127.4, 126.1, 61.2, 14.5.

1,3,5-tris(1-naphthyl)benzene (2q, Ref. 19**)**

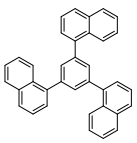

The molecule was purified by column chromatography using hexane as eluent followed by recrystallization (hexane/ethyl acetate) of the isolated product. White solid (41%, 312 mg). m. p.

196-197 °C; ^{1}H-NMR (500 MHz, $CDCl_3$) δ 8.20 (d, *J* = 8.6 Hz, 3H), 7.91-7.93 (m, 3H), 7.88 (d, *J* = 8.6 Hz, 3H), 7.75 (s, 3H), 7.61 (dd, *J* = 7.4, 1.1 Hz, 3H), 7.55 (t, *J* = 7.4 Hz, 3H), 7.47-7.51 (m, 6H). ^{13}C{^{1}H}-NMR (125 MHz, $CDCl_3$) δ 140.9, 139.9, 134.0, 131.7, 130.8, 128.5, 128.0, 127.4, 126.4, 126.1, 126.0, 125.6.

6. Synthesis of Hexa-peri-benzocoronene (5)

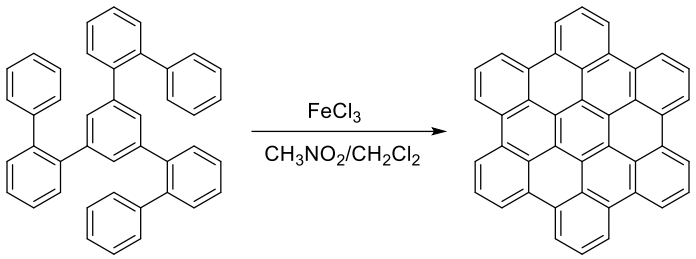

2o **5**

The compound **5** was prepared by following the literature procedure (ref. 20). 10 mg of **2o** (0.0184 mmol) was dissolved in 8 ml of dichloromethane, the solution was degassed by bubbling through argon for 10 min, and then 100 mg of $FeCl_3$ in 0.4 mL of CH_3NO_2 was added dropwise. After being stirred for 1 h, the reaction was quenched by adding 10 ml of methanol, the yellow precipitate was collected, washed by methanol repeatedly and dried under vacuum to afford 7.2 mg of yellow powder (76%). MALDI-TOF: 522.19, cal. ($C_{42}H_{18}$) 522.14.

7. Reaction Procedure for *p*-BCOTPB (4) Synthesis

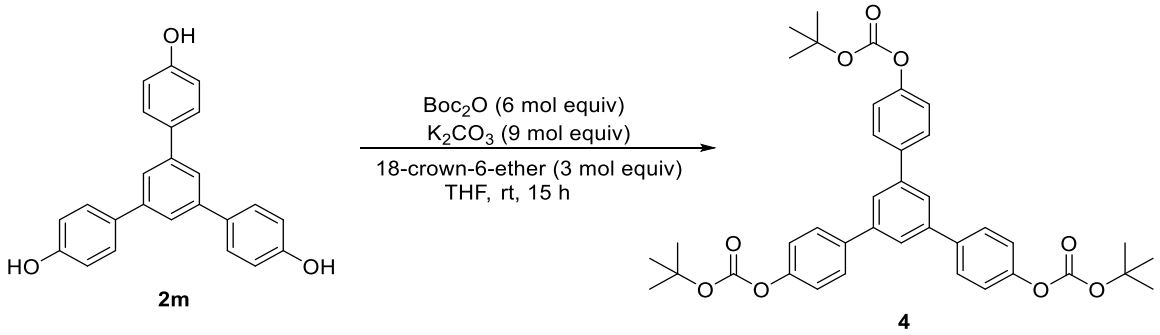

2m **4**

A mixture of **2m** (90 mg, 0.25 mmol, 1 mol equiv), BOC_2O (350 mg, 1.5 mmol, 6 mol equiv), 18-crown-6-ether (200 mg, 0.75 mmol, 3 mol equiv) and K_2CO_3 (316 mg, 2.3 mmol, 9 mol equiv) were taken in a round bottomed flask and degassed under vacuum and then refill with nitrogen (3 times). After that 10 mL of THF was added to the reaction mixture. The reaction mixture was stirred at room temperature for overnight (15 h). After the completion of reaction, the mixture was diluted with ethyl acetate and extracted with water and brine. The organic layer was collected and dried over Na_2SO_4. The ethylacetate was removed by using a rotary evaporator. Finally, the crude mixture was purified by column chromatography (hexane/ethyl acetate = 10:1)

1,3,5-tris(4-*t*-butoxycarbonyloxyphenyl)benzene (4, Ref. 21**)**

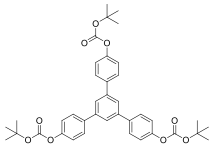

White solid (86%, 142 mg). m. p. 120-122 °C; ^{1}H-NMR (500 MHz, $CDCl_3$) δ 7.69 (s, 3H), 7.66 (dd, *J* = 6.8, 2.4 Hz, 6H), 7.28 (dd, *J* = 6.8, 2.4 Hz, 6H), 1.58 (s, 27H). ^{13}C{^{1}H}-NMR (125 MHz, $CDCl_3$) δ 152.8, 150.8, 141.7, 138.6, 128.4, 125.2, 121.8, 83.8, 27.8.

8. Procedure for Multigram-Scale Reaction

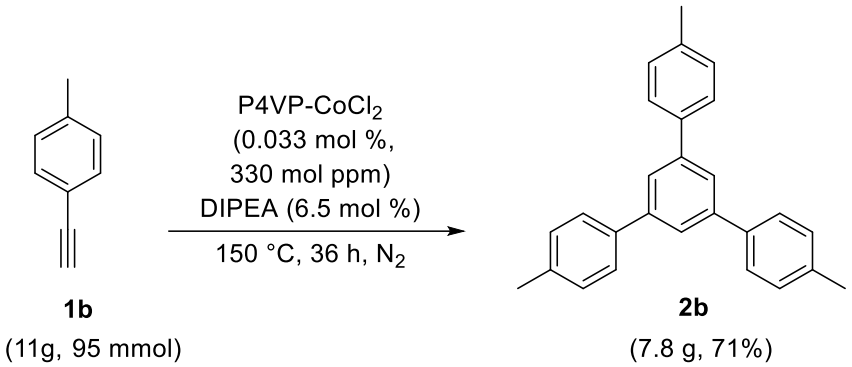

A mixture of P4VP-$CoCl_2$ (330 mol ppm, 35 mg), 1-ethynyl-4-methylbenzene **1b** (1 mol equiv, 95 mmol, 11g), and DIPEA (6.5 mol %, 798 mg) were added to a 50 mL round bottomed flask. The reaction system was connected with a condenser and degassed under vacuum and refilled with N_2 under standard Schlenk techniques (3 times). Next, the round bottomed flask was placed over an oil bath at 150 °C (set temperature 160 °C) under nitrogen for 36 h. After the reaction, the reaction mixture was diluted by EtOAc. The solid catalyst was filtered and washed with EtOAc and methanol. Finally, the collected recovered catalyst was dried under vacuum (34.3 mg). On the other side, the EtOAc solution (filtrate) was also collected. The solvent was evaporated under vacuum and crude mass was purified by column chromatography to give product **2b** (71%, 7.8 g).

9. Catalyst Recovery and Application of Recovered Catalyst

9.1. Flow Chart for Catalyst Recovery

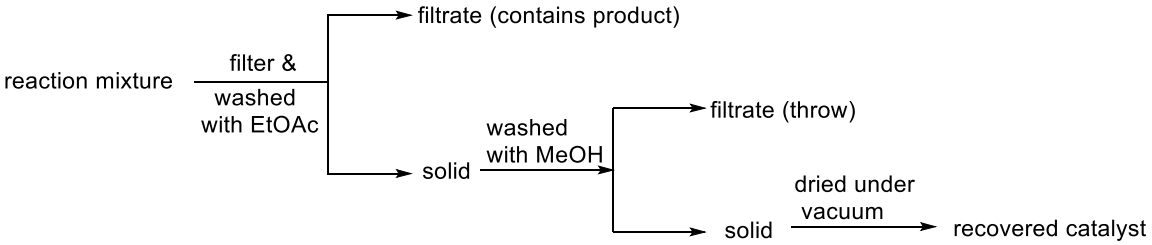

9.2. Application of Recovered Catalyst in Cyclotrimerization Reaction

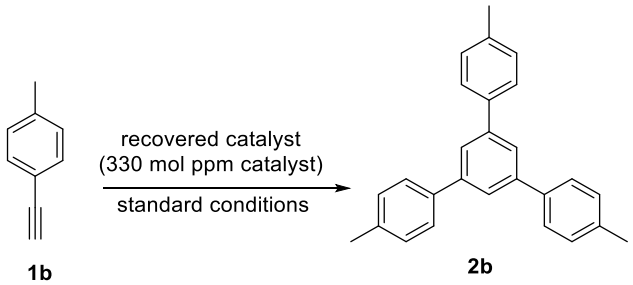

entry	number of run	catalyst recovery yield (%)	yield of **2b** (%)
1	1st	98	84
2	2nd	95	80
3	3rd	97	72

9.3. Hot Filtration Test

A mixture of P4VP-$CoCl_2$ (330 mol ppm, 1.85 mg), aryl alkyne, **1** (1 mol equiv, 5 mmol), and DIPEA (6.5 mol %, 42 mg) were added to a reaction tube. The reaction tube was degassed under vacuum and refilled with N_2 under standard Schlenk techniques (3 times). The reaction tube was sealed with screw cap and Teflon then placed over a chemiStation (metal block) under nitrogen for 3 h. A small portion of the reaction mixture was taken out for NMR analysis. The remaining portion was immediately filtered through a Milipore filter paper and washed with hot xylene. Nitrogen gas was passed through the solution for 10 minutes. After that, the reaction system was sealed and placed over a chemiStation at 150 °C for another 24 h. After 24 h the reaction mixture was removed from the chemiStation and diluted with ethyl acetate. The yield was determined by the crude NMR analysis using 1,3,5-trimethoxybenzene as an internal standard.

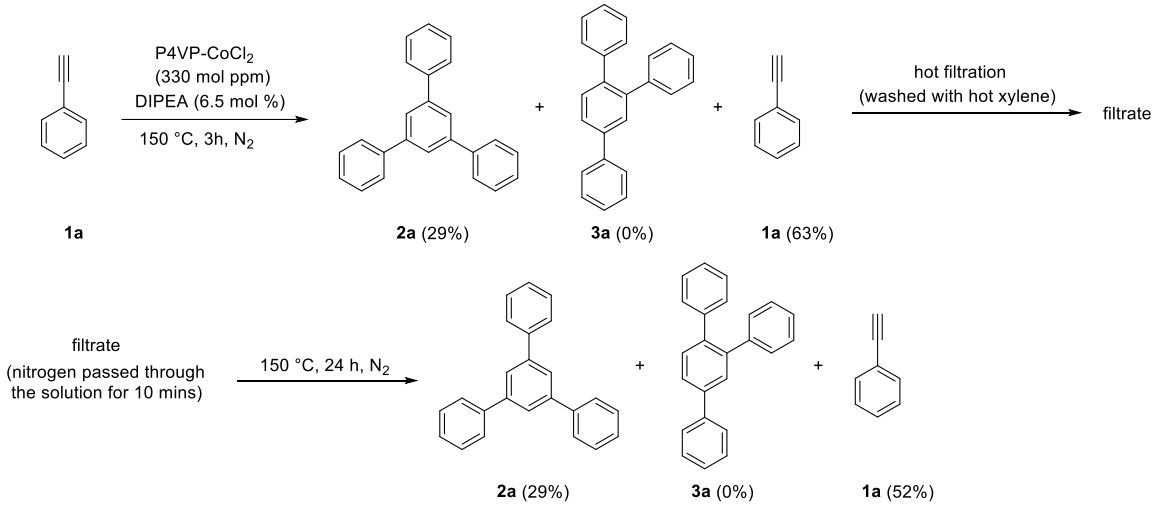

10. Effects of Different Ratio of Poly(4-vinylpyridine) and Cobalt Chloride

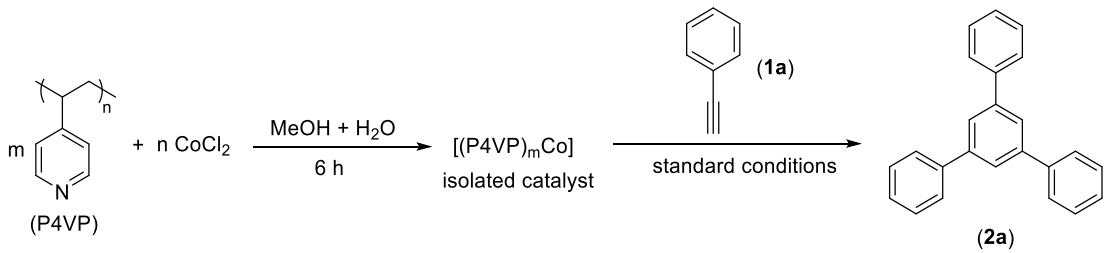

Poly(4-vinylpyridine), P4VP (average M_w = 160000, Aldrich) was dissolved in 10 mL of methanol. An aqueous solution (10 mL) of $CoCl_2$ was slowly added to the polymer containing methanol solution. The reaction mixture was stirred for 6 h at room temperature. After that, the precipitate was filtered and the filtrate was discarded. The residue was washed with water (3x10 mL), methanol (4x10 mL), and diethyl ether (5x5 mL). Next, the residue was collected and dried over vacuum for overnight (15 h) to get polymer supported cobalt catalyst. A mixture of cobalt catalyst (1.85 mg), phenylacetylene, **1a** (1 equiv, 5 mmol), and DIPEA (6.5 mol%, 42 mg) were added to a reaction tube. The reaction tube

was degassed under vacuum and refilled with N_2 under standard Schlenk techniques (3 times). The reaction tube was sealed with screw cap and teflon then placed over a chemiStation under nitrogen for 24 h. After the reaction, the reaction mixture was diluted by EtOAc and filtered through a celite pad, and washed with EtOAc. The EtOAc solution was collected to measure the yield of **2a** from the NMR analysis by using 1,3,5-trimethoxybenzene as an internal standard.

entry	Co:N (n:m)	wt% yield of catalyst	yield of **2a** (%)
1	2:1	6	10
2	1:1	17	7
3	1:2	43	69
4	1:3	41	64
5	1:4	67	39

11. ICP-MS Analysis

Inductively coupled plasma mass spectrometry **(**ICP-MS) measurement was performed using Perkin Elmer Nexion 300D. The sample was pretreated by microwave digestion technique with high-purity nitric acid (7 mL, 69%, obtained from Kanto Chemical, Ultrapur-100 grade) and hydrogen peroxide (1 mL, 30-32%, obtained from Kanto Chemical, Ultrapur grade) as solvent using Perkin Elmer Titan MPS microwave sample preparation system. A cobalt standard solution was obtained from Merck.

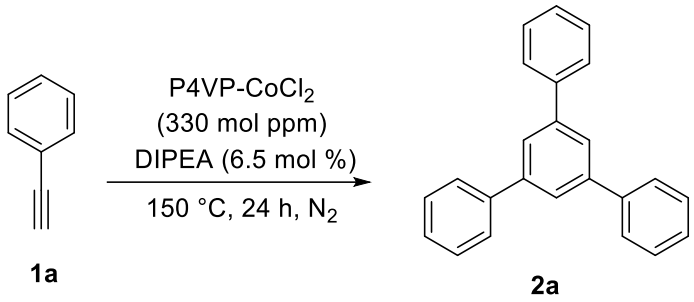

ICP-MS Analysis of Cobalt in 2a

Solid product **2a** (34 mg) was heated with nitric acid and hydrogen peroxide using a microwave heating system, and the resulted solution was diluted with water to 200 mL total. ICP-MS analysis of the solution showed that 0.03 mg Kg^{-1} (0.03 ppm) of cobalt contaminated to the solid product (the limit of detection of ICP-MS: 0.01 mg Kg^{-1}).

12. Effect of Base on Catalyst Reusability

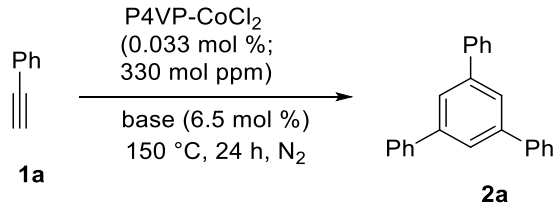

entry	base	fresh yield of **2a** (%)	1st reuse yield **2a** (%)
1	Et_3N	39	12
2	DIPEA	69	65
3	no base	64	14
4	K_3PO_4	0	0
5	KO^tBu	0	0

13. XPS Analysis of Catalyst and Recovered Catalyst

XPS studies were performed with the catalyst recovered from the multi-gram-scale reaction. The studies were performed after the argon etching (one time) to clear the surface of the catalyst and recovered catalyst. The spectra's of the recovered catalyst showed similar pattern with the spectra's of original P4VP-Co (II) catalyst. The 2p level XPS spectra for recovered catalyst (Figure S4c) as well as the original catalyst (figure S4a) only showed the presence of +2 oxidation states of cobalt.

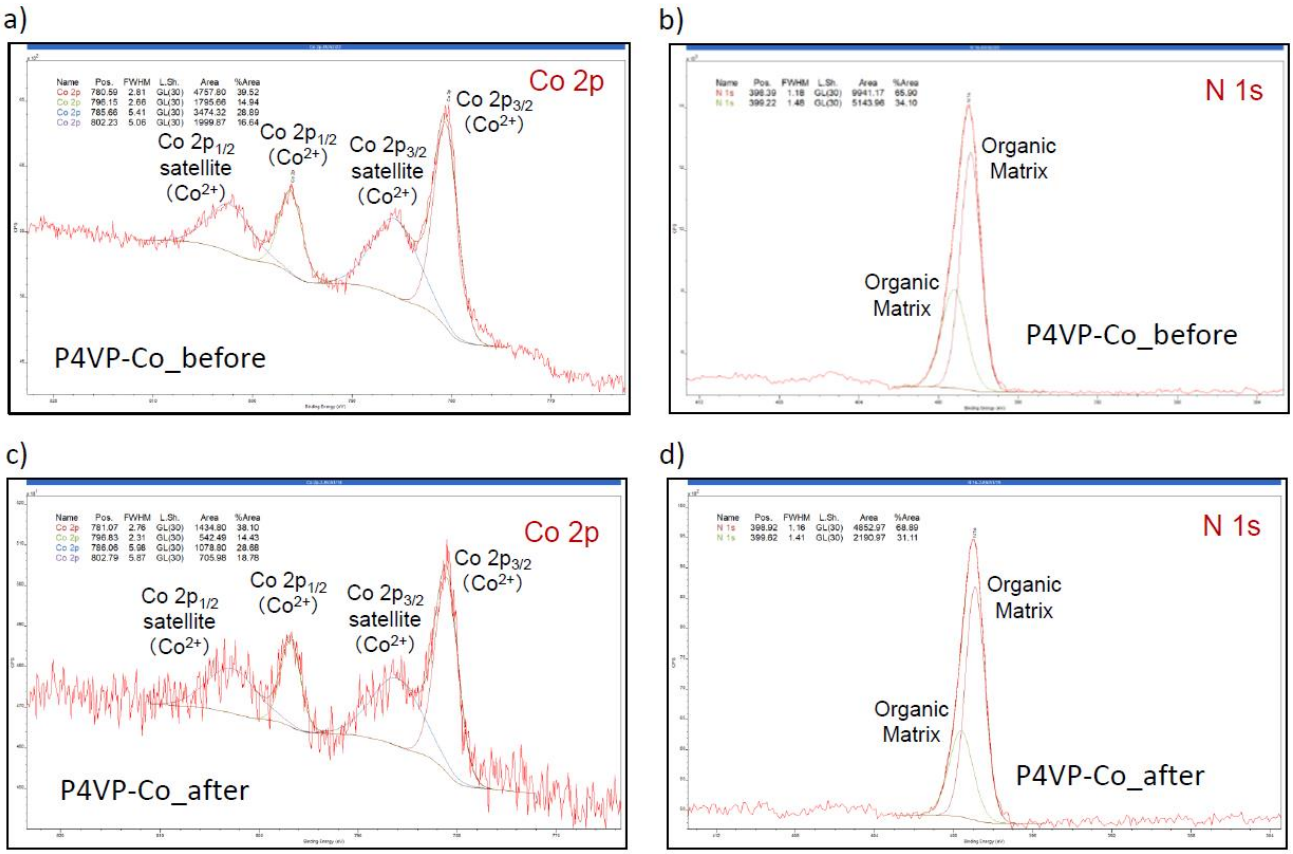

Figure S4. a) XPS spectra of cobalt 2p orbital of P4VP-Co catalyst before reaction. b) XPS spectra of nitrogen 1s orbital of P4VP-Co catalyst before reaction. c) XPS spectra of cobalt 2p orbital of P4VP-Co catalyst after reaction (recovered catalyst). d) XPS spectra of nitrogen 1s orbital of P4VP-Co catalyst after reaction (recovered catalyst).

14. Speculative Origin of Selectivity

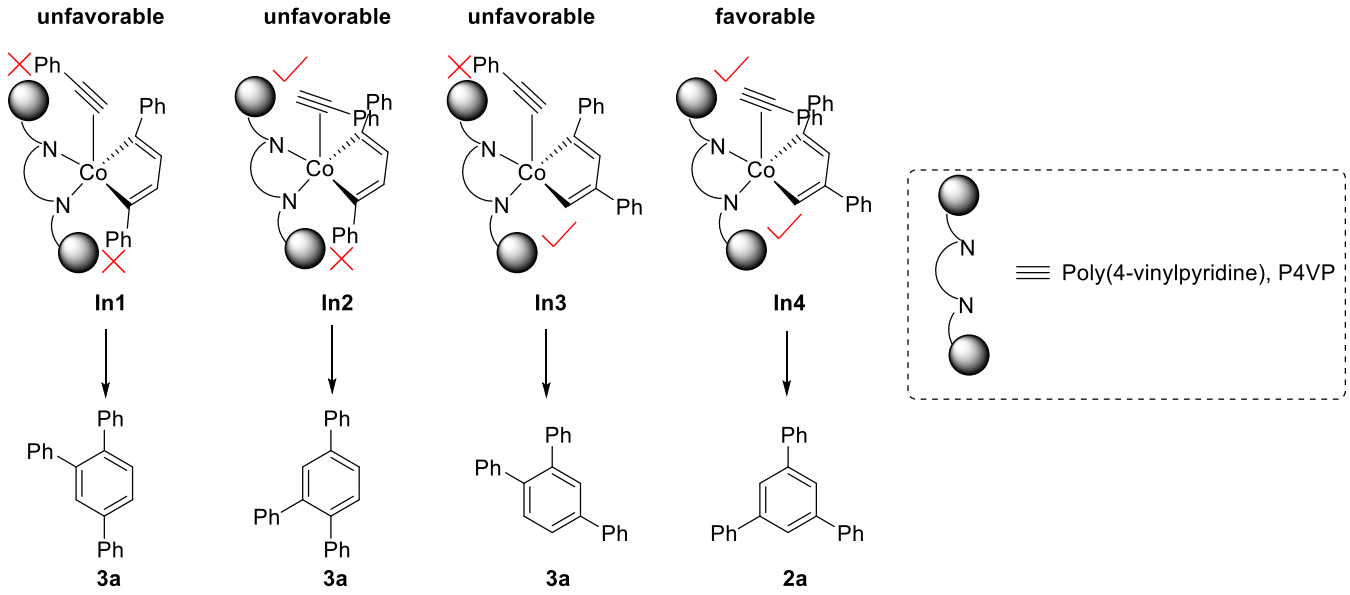

Figure S5. Speculative Origin of Selectivity

The cobaltacycle intermediate (**In1**, **In2**, and **In3**) will provide the 1,2,4-triphenylbenzene (**3a**) whereas the cobaltacycle intermediate **In4** will provide the desired 1,3,5-triphenylbenzene (**2a**). A steric hindrance between the polymer chain unit and the phenyl ring (**1a**) in the case of **In1**, **In2,** and **In3** makes these three cobaltacycles unfavorable. There is no such steric hindrance in **In4** which is expected to deliver the product with exclusive selectivity. A π-π stacking interaction between the phenyl groups may stabilize the intermediates **In2** and **In4** but **In2** suffers from steric destabilization too. So, **In4** is the most favored intermediate.

15. The Major Side-Product Obtained from the Reaction

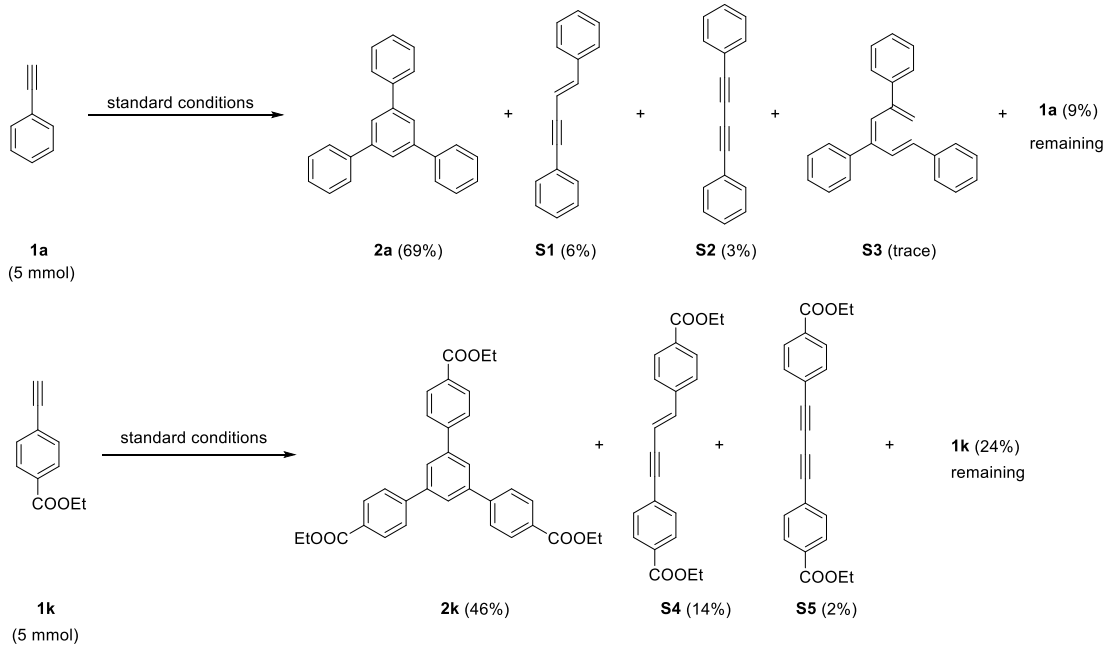

16. Reference

1. Feng, L.; Hu, T.; Zhang, S.; Xiong, H.-Y.; Zhang, G. Copper-Mediated Deacylative Coupling of Ynones via C-C Bond Activation Under Mild Conditions. *Org. Lett.* **2019**, *21*, 9487.
2. Yang, X.; Jin, X.; Wang, C. Manganese-Catalyzed ortho-C-H Alkenylation of Aromatic N-H Imidates with Alkynes: Versatile Access to Mono-Alkenylated Aromatic Nitriles. *Adv. Synth. Catal.* **2016**, *358*, 2436.
3. Cheung, K. P. S.; Tsui, G. C. Copper(I)-Catalyzed Interrupted Click Reaction with $TMSCF_3$: Synthesis of 5-Trifluoromethyl 1,2,3-Triazoles. *Org. Lett.* **2017**, *19*, 2881.
4. Sha, F.; Alper, H. Ligand- and Additive-Controlled Pd-Catalyzed Aminocarbonylation of Alkynes with Aminophenols: Highly Chemo- and Regioselective Synthesis of α, β -unsaturated Amides. *ACS Catal.* **2017**, *7*, 2220.
5. Song, C.; Dong, X.; Wang, Z.; Liu, K.; Chiang, C.-W.; Lei, A. Visible-Light-Induced [4+2] Annulation of Thiophenes and Alkynes to Construct Benzene Rings. *Angew. Chem., Int. Ed.* **2019**, *58*, 12206.
6. Bao, H.; Zhou, B.; Luo, S.-P.; Xu, Z.; Jin, H.; Liu, Y. P/N Heteroleptic Cu(I)-Photosensitizer-Catalyzed Deoxygenative Radical Alkylation of Aromatic Alkynes with Alkyl Aldehydes Using Dipropylamine as a Traceless Linker Agent. *ACS Catal.* **2020**, *10*, 7563.
7. Dutta, U.; Maity, S.; Kancherla, R.; Maiti, D. Aerobic Oxynitration of Alkynes with *t*BuONO and TEMPO. *Org. Lett.* **2014**, *16*, 6302.
8. Margaux, E.; Michael, W. D.; Florent, D. M.; Fabien, S.; Jean-Francois, L.; Robert, P. B.; Jean-Luc, R.; Matthieu, H.; Mathieu, L.; Ruben, R. D.; Sylvain, G. Role of the Bridging Group in Bis-Pyridyl Ligands: Enhancing Both the Photo- and Electroluminescent Features of Cationic (IPr)CuI Complexes. *Chem. Eur. J*, **2017**, *23*, 16328.
9. Ravel, B.; Newville, M. ATHENA, ARTEMIS, HEPHAESTUS: Data Analysis for X-Ray Absorption Spectroscopy Using IFEFFIT. *J. Synchrotron Rad.* **2005**, *12*, 537.
10. Zabinsky, S. I.; Rehr, J. J.; Ankudinov, A.; Albers, R. C.; Eller, M. J. Multiple-Scattering Calculations of X-Ray-Absorption Spectra. *Phys. Rev. B* **1995**, *52*, 2995.
11. a) Neese, F. The ORCA Program System. *WIRs Comput. Mol. Sci.* **2012**, *2*, 73; b) Neese, F. Software Update: the ORCA Program System, version 4.0. *WIRs Comput. Mol. Sci.* **2018**, *8*, 1327.
12. a) Grimme, S.; Ehrlich, S.; Goerigk, L. J. Effect of the Damping Function in Dispersion Corrected Density Functional Theory. *Comput. Chem.* **2011**, *32*, 1456. b) Grimme, S.; Antony, J.; Ehrlich, S.; Krieg, H. A Consistent and Accurate ab initio Parametrization of Density Functional Dispersion Correction (DFT-D) for the 94 Elements H-Pu. *J. Chem. Phys.* **2010**, *132*, 154104.
13. Saha, A.; Wu, C.-M.; Peng, R.; Koodali, R.; Banerjee, S. Facile Synthesis of 1,3,5-Triarylbenzenes and 4-Aryl-NH-1,2,3-Triazoles Using Mesoporous Pd-MCM-41 as Reusable Catalyst. *Eur. J. Org. Chem.* **2019**, 104.
14. Yang, K.; Wang, P.; Sun, Z.-Y.; Guo, M.; Zhao, W.; Tang, X.; Wang, G. Hydrogen-Bonding Controlled Nickel-Catalyzed Regioselective Cyclotrimerization of Terminal Alkynes. *Org. Lett.* **2021**, *23*, 3933.

15. Xi, C.; Sun, Z.; Liu, Y. Cyclotrimerization of Terminal Alkynes Catalyzed by the System of $NiCl_2$/Zn and (Benzimidazolyl)- 6-(1-(Arylimino)ethyl)pyridines. *Dalton Trans*. **2013**, *42*, 13327.
16. Tayebee, R.; Savoji, K.; Razib, M. K.; Maleki, B. Environmentally Friendly Cyclotrimerization of Substituted Acetophenones Catalyzed by a New Nanocomposite of γ-Al_2O_3 Nanoparticles Decorated with $H_5PW_{10}V_2O_{40}$. *RSC Adv*., **2016**, *6*, 55319.
17. Deng, K.; Huai, Q.-Y.; Shen, Z.-L.; Li, H. J.; Liu, C.; Wu, Y. C. Rearrangement of Dypnones to 1,3,5-Triarylbenzenes. *Org*. *Lett*. **2015**, *17*, 1473.
18. Zhang, S.-L.; Xue, Z.-F.; Gao, Y.-R.; Mao, S.; Wang, Y.-Q. Triple Condensation of Aryl Methyl Ketones Catalyzed by Amine and Trifluoroacetic Acid: Straightforward Access to 1,3,5-Triarylbenzenes under Mild Conditions. *Tetrahedron Lett*. **2012**, *53*, 2436.
19. Joosten, A.; Soueidan, M.; Denhez, C.; Harakat, D.; Hélion, F.; Namy, J.-L.; Vasse, J. L.; Szymoniak, J. Multimetallic Zirconocene-Based Catalysis: Alkyne Dimerization and Cyclotrimerization Reactions. *Organometallics* **2008**, *27*, 4152.
20. Feng, X.; Wu, J.; Enkelmann, V.; Müllen, K. Hexa-peri-hexabenzocoronenes by Efficient Oxidative Cyclodehydrogenation-the Role of the Oligophenylene Precursors. *Org*. *Lett*. **2006**, *8*, 1145.
21. Kadota, T.; Kageyama, H.; Wakaya, F.; Gamo, K.; Shirota, Y. Novel Electron-Beam Molecular Resists with High Resolution and High Sensitivity for Nanometer Lithography. *Chem*. *Lett*. **2004**, *33*, 706.

17. Product NMR

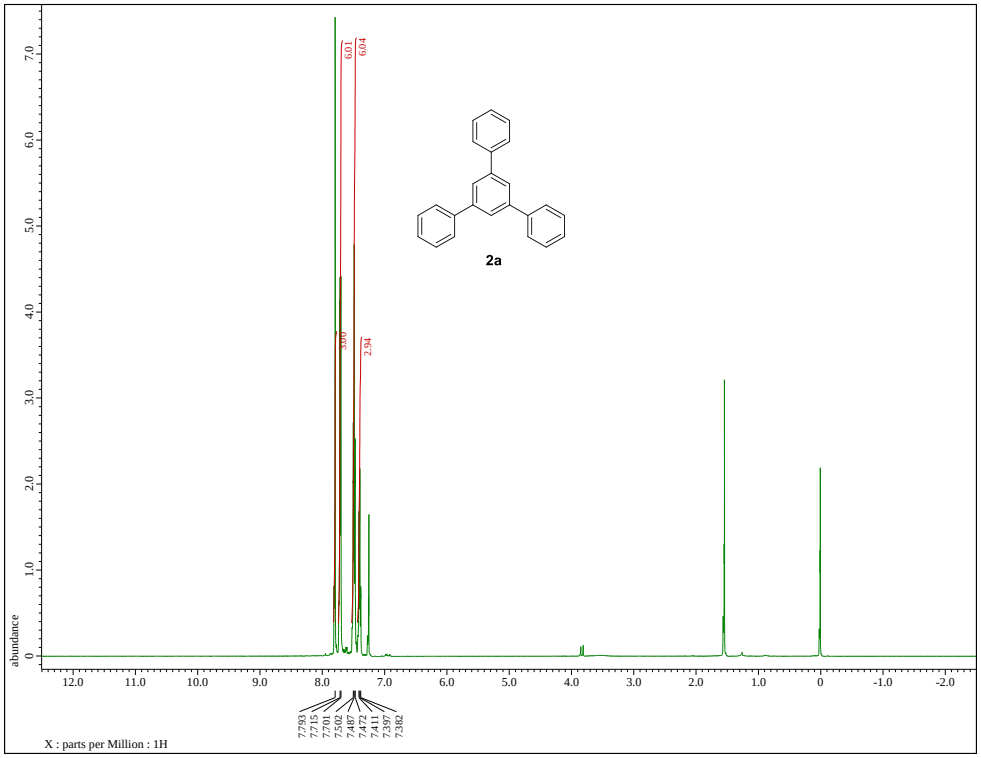

Figure S6-1. ^{1}H-NMR spectrum of compound **2a** (500 MHz, $CDCl_3$)

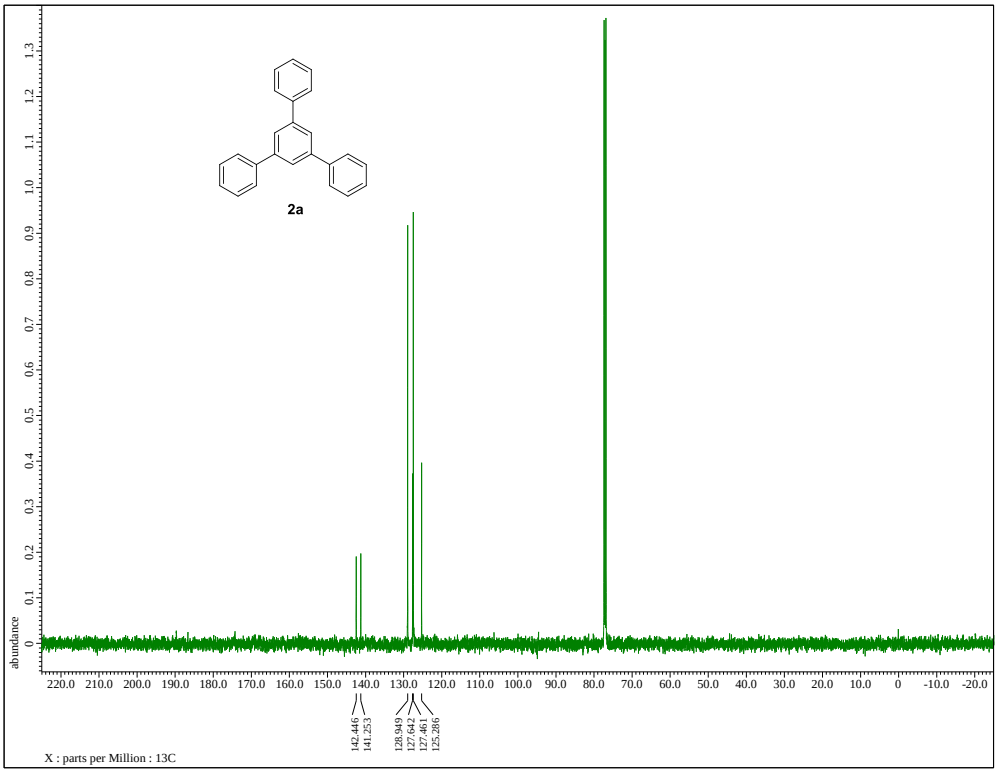

Figure S6-2. $^{13}C\{^{1}H\}$-NMR spectrum of compound **2a** (125 MHz, $CDCl_3$)

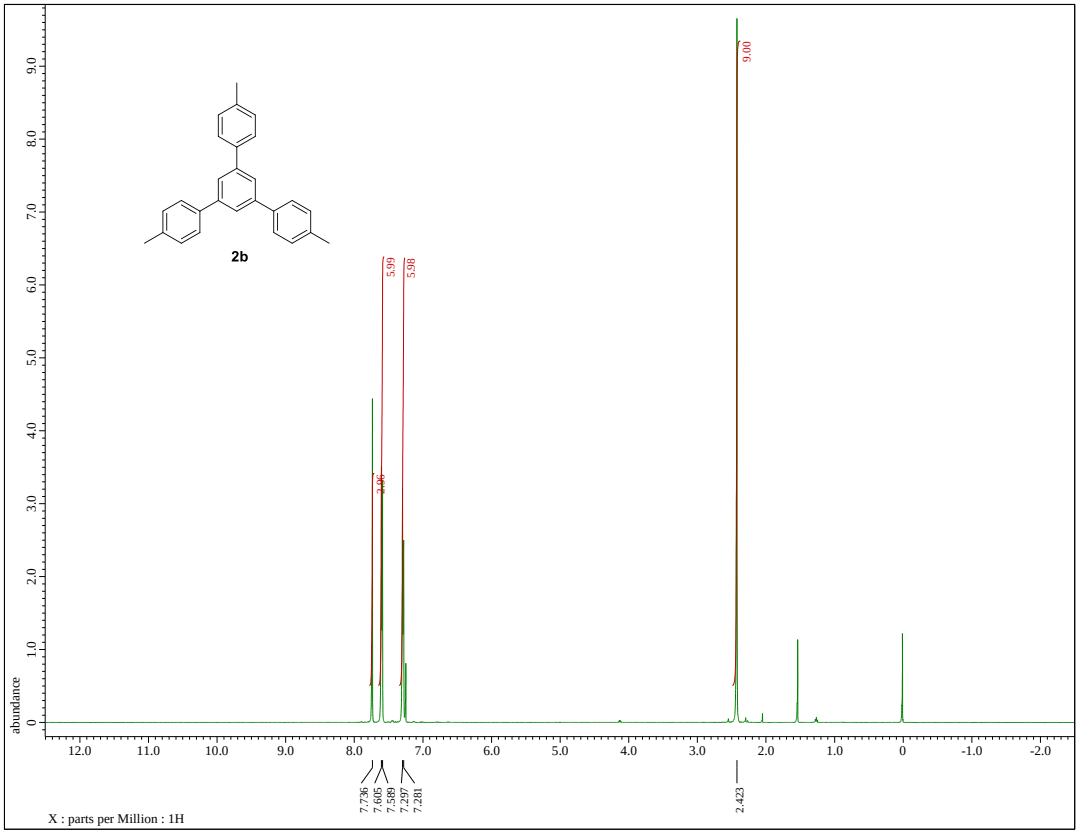

Figure S7-1. ^{1}H-NMR spectrum of compound **2b** (500 MHz, $CDCl_3$)

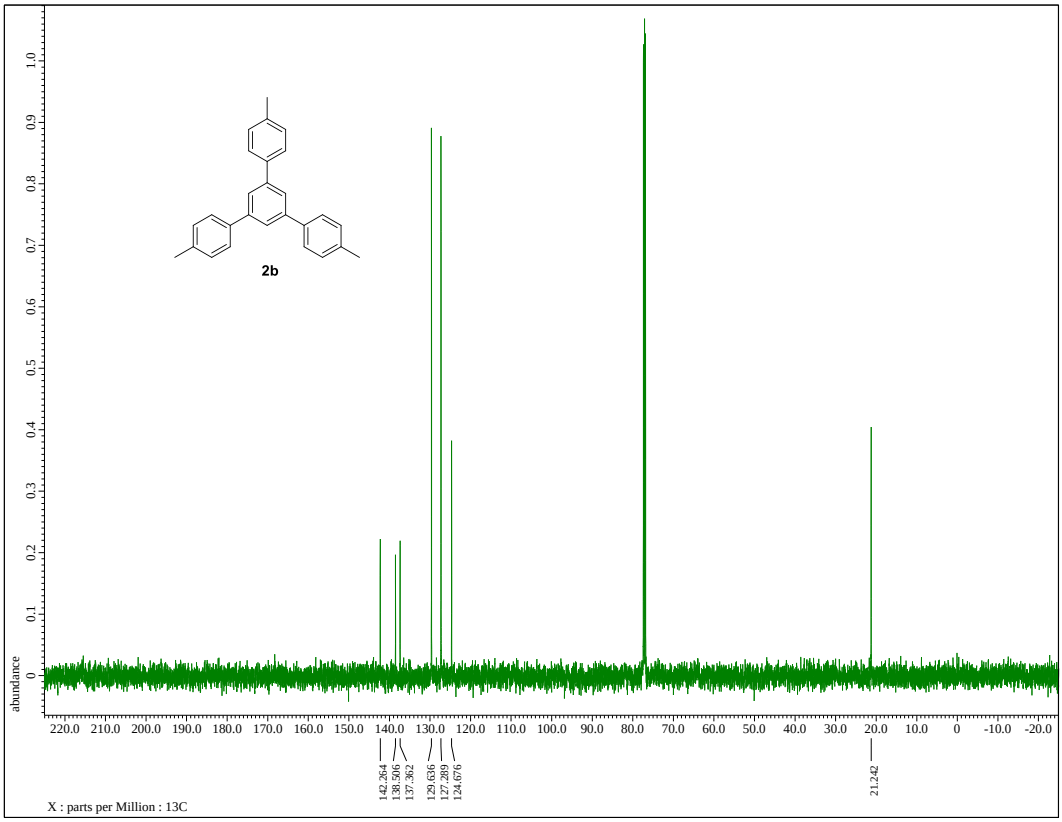

Figure S7-2. $^{13}C\{^{1}H\}$-NMR spectrum of compound **2b** (125 MHz, $CDCl_3$)

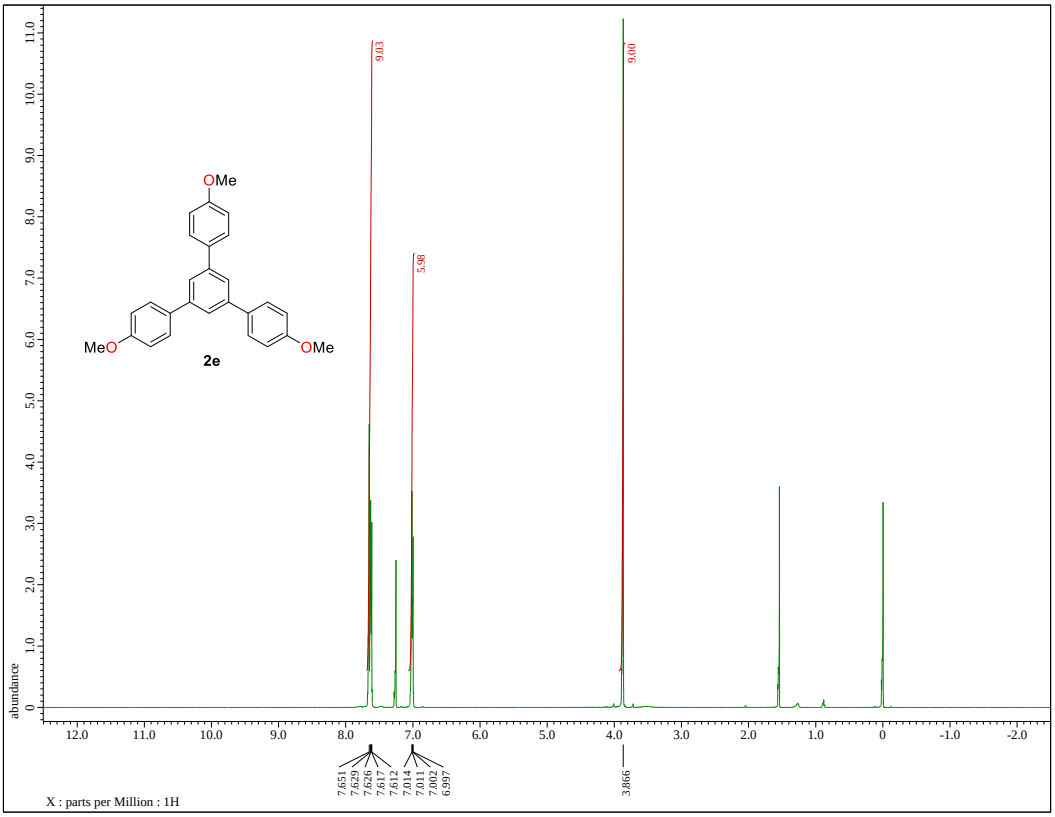

Figure S8-1. ^{1}H-NMR spectrum of compound **2e** (500 MHz, $CDCl_3$)

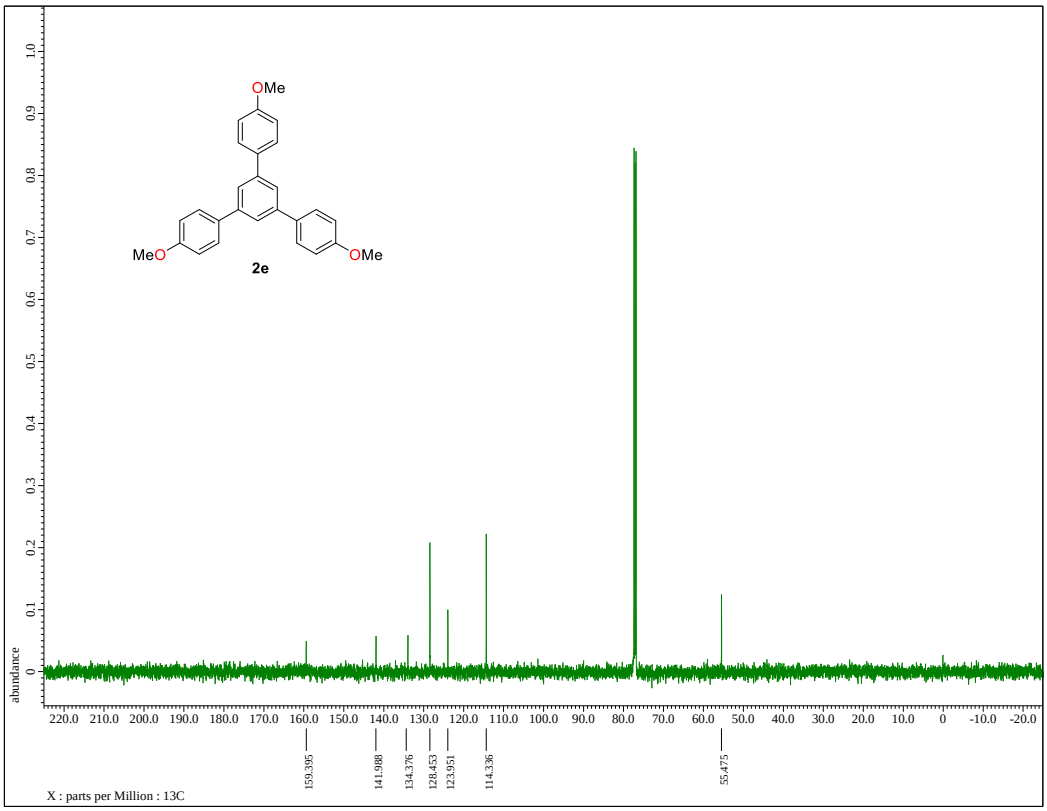

Figure S8-2. $^{13}C\{^{1}H\}$-NMR spectrum of compound **2e** (125 MHz, $CDCl_3$)

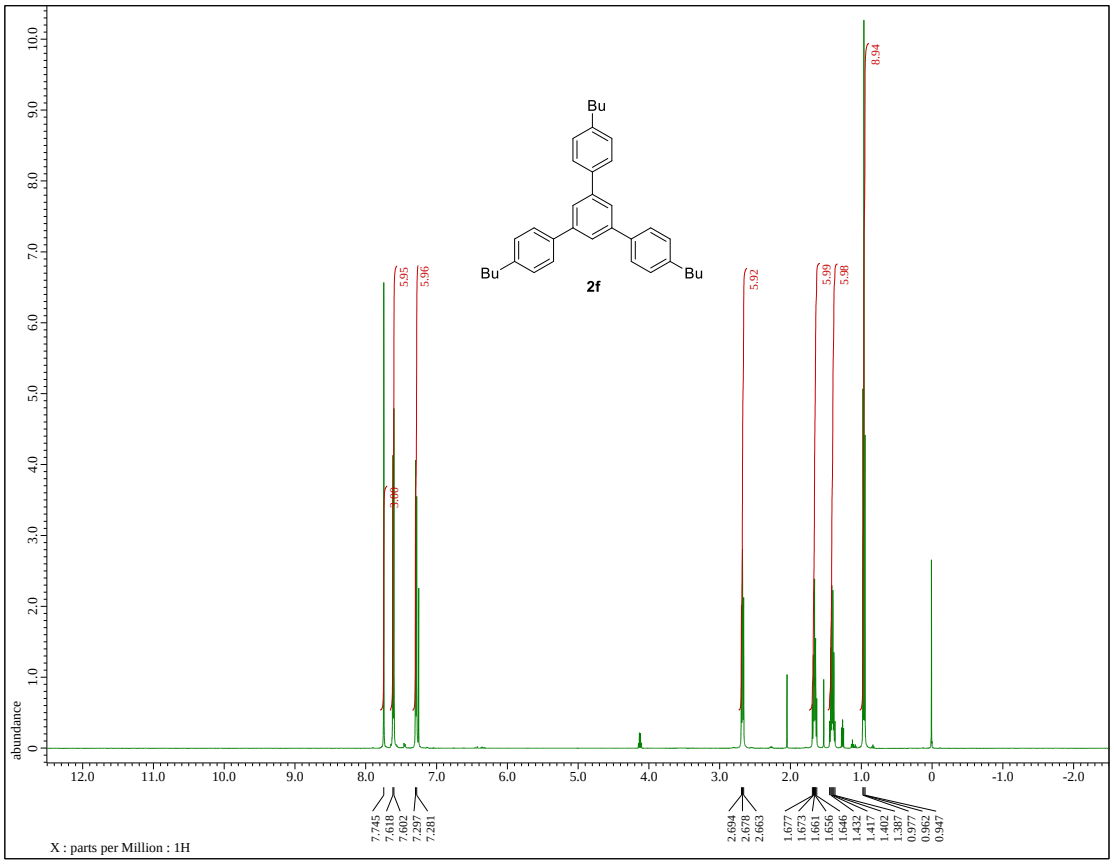

Figure S9-1. ^{1}H-NMR spectrum of compound **2f** (500 MHz, $CDCl_3$)

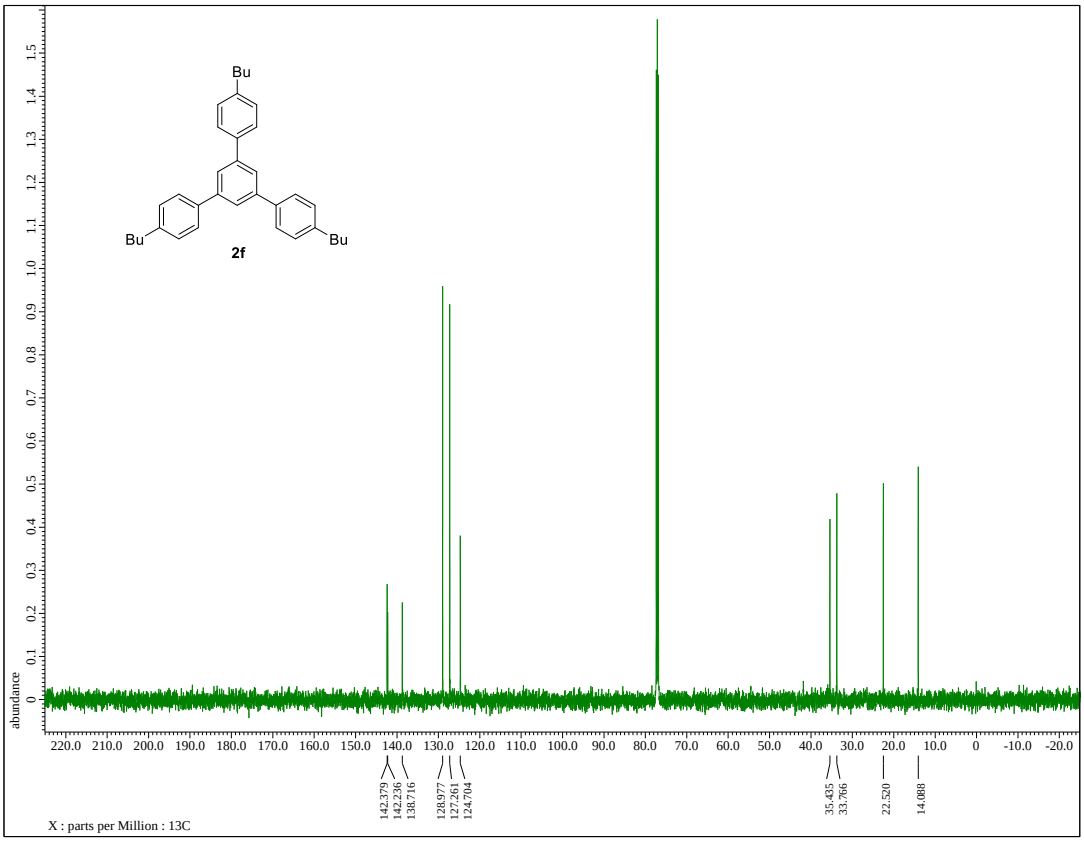

Figure S9-2. ^{13}C{^{1}H}-NMR spectrum of compound **2f** (125 MHz, $CDCl_3$)

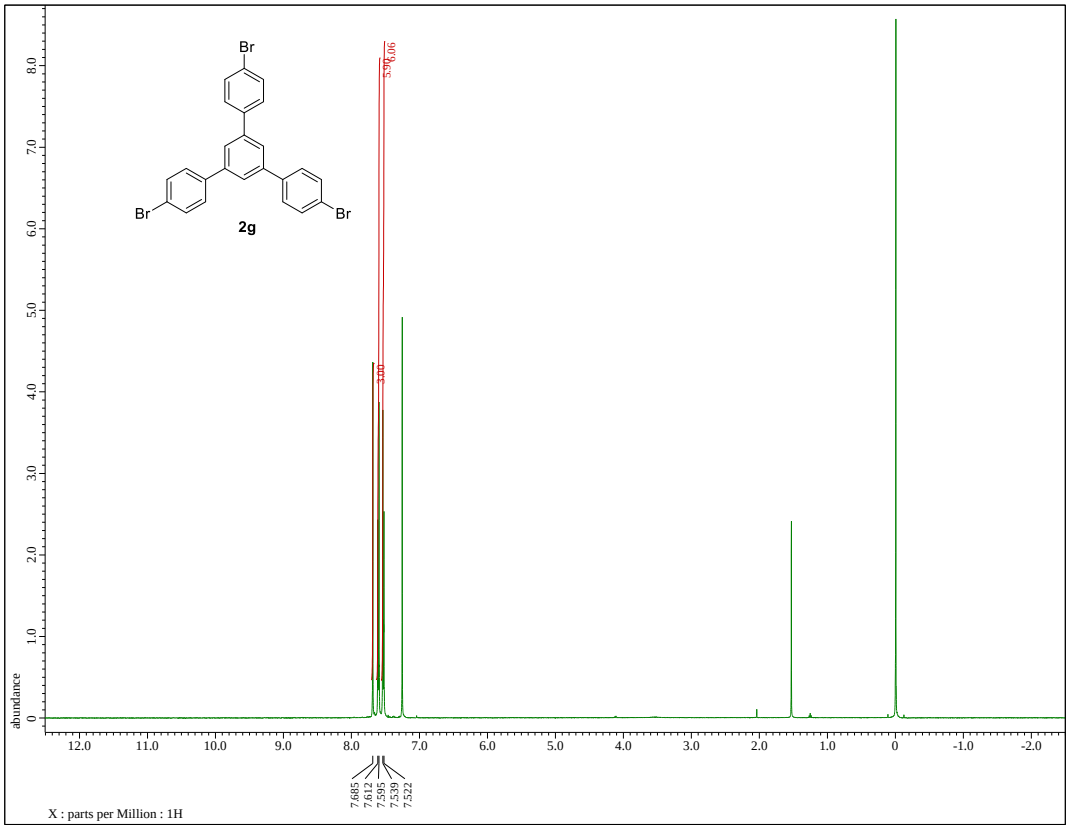

Figure S10-1. ^{1}H-NMR spectrum of compound **2g** (500 MHz, $CDCl_3$)

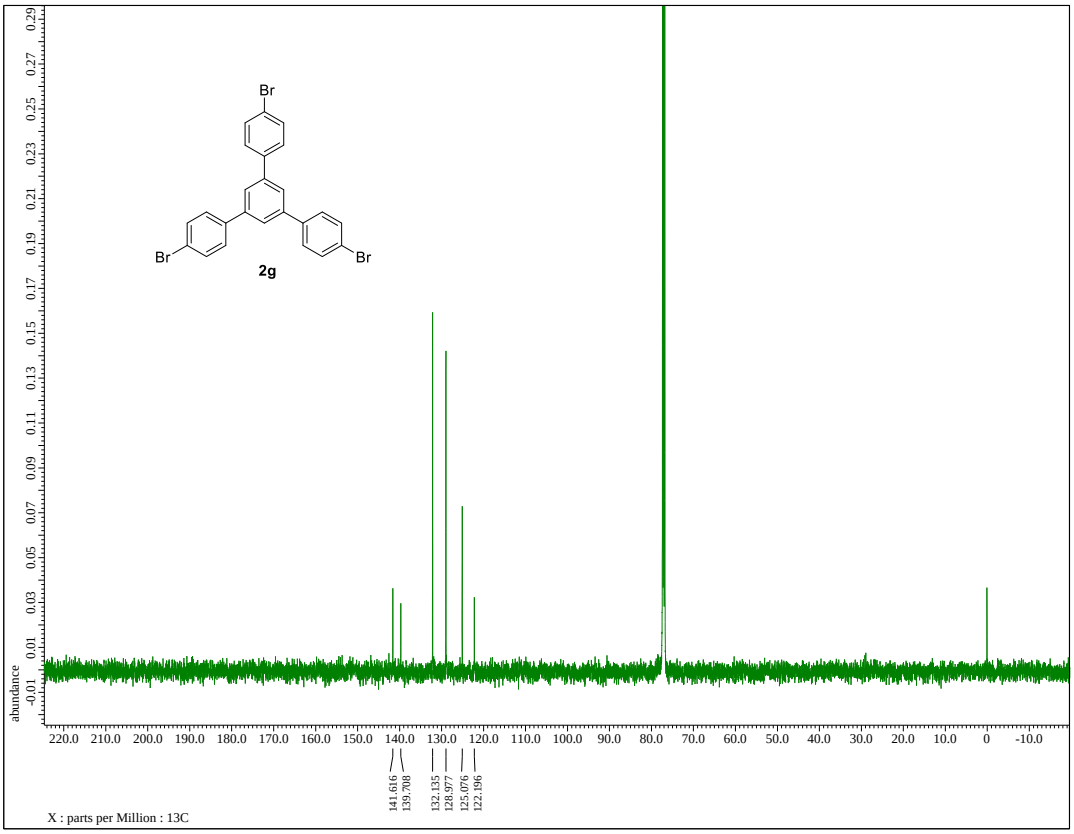

Figure S10-2. $^{13}C\{^{1}H\}$-NMR spectrum of compound **2g** (125 MHz, $CDCl_3$)

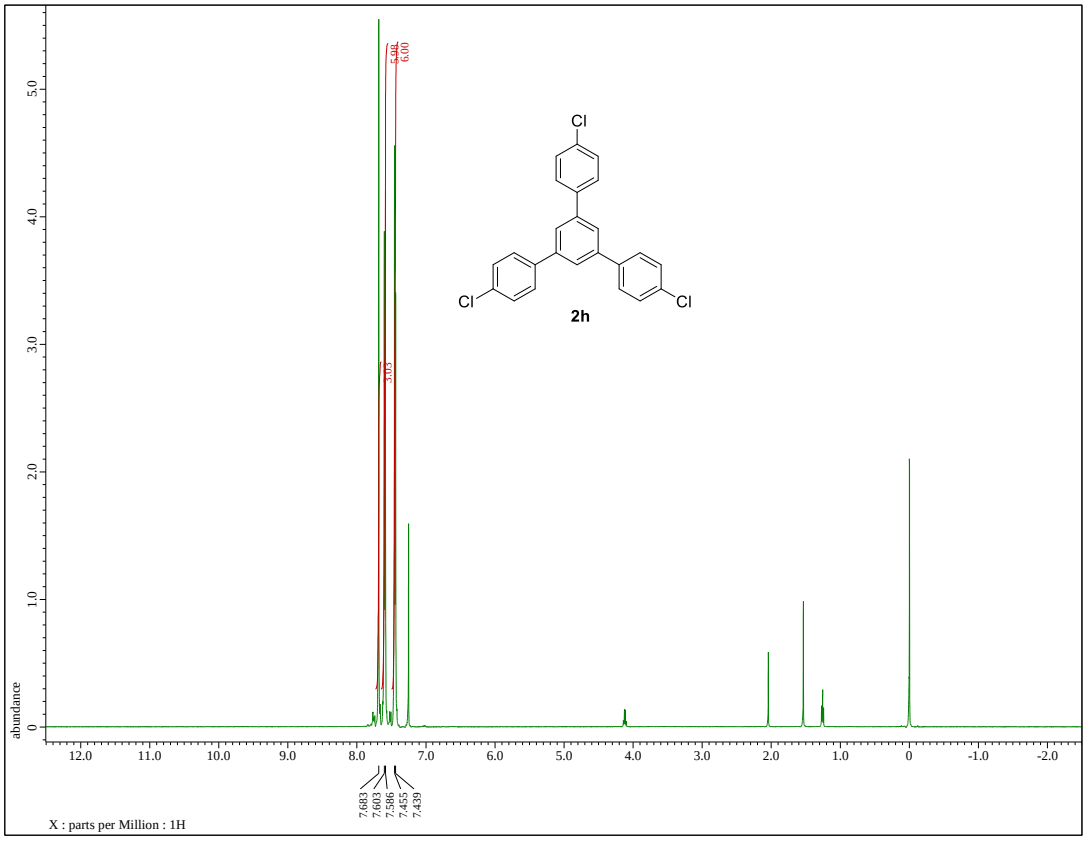

Figure S11-1. ^{1}H-NMR spectrum of compound **2h** (500 MHz, $CDCl_3$)

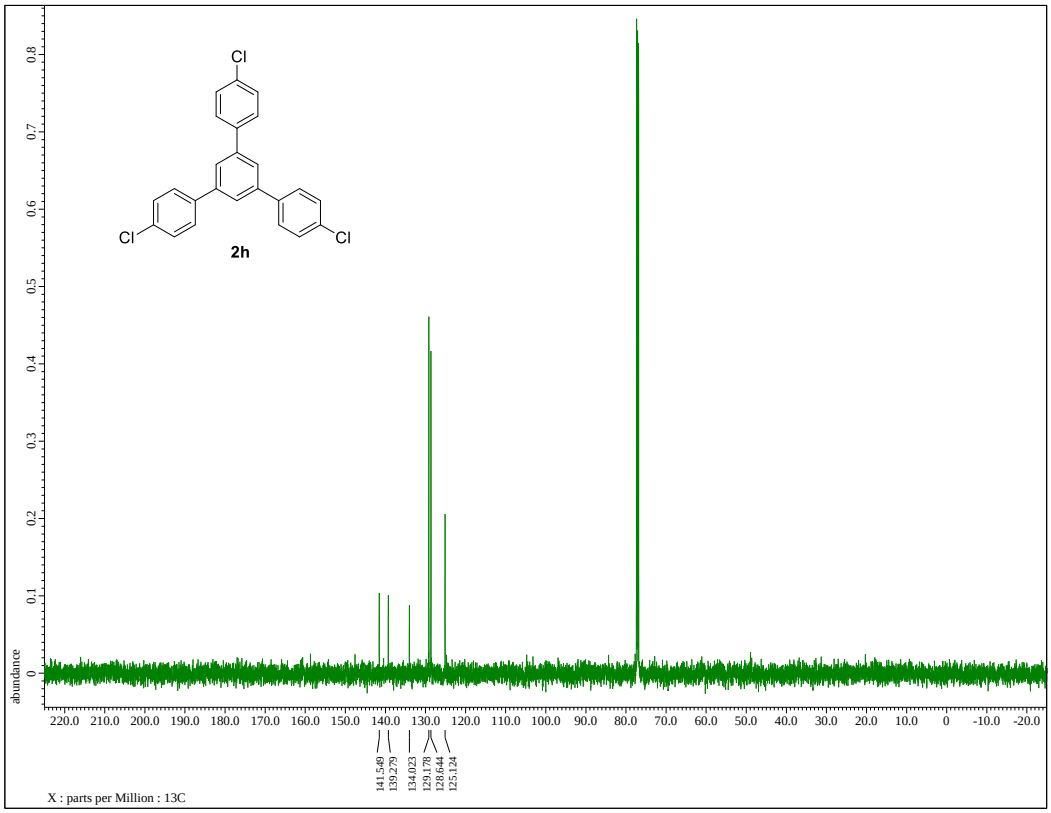

Figure S11-2. $^{13}C\{^{1}H\}$-NMR spectrum of compound **2h** (125 MHz, $CDCl_3$)

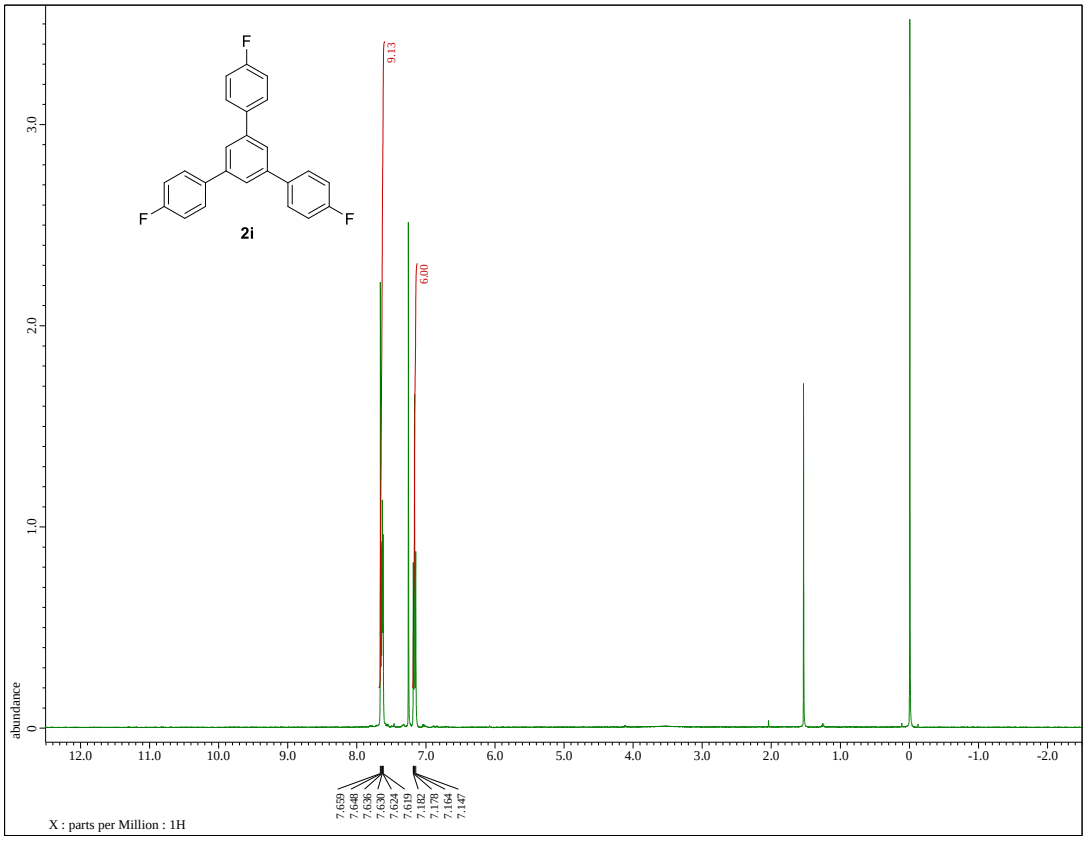

Figure S12-1. ^{1}H-NMR spectrum of compound **2i** (500 MHz, $CDCl_3$)

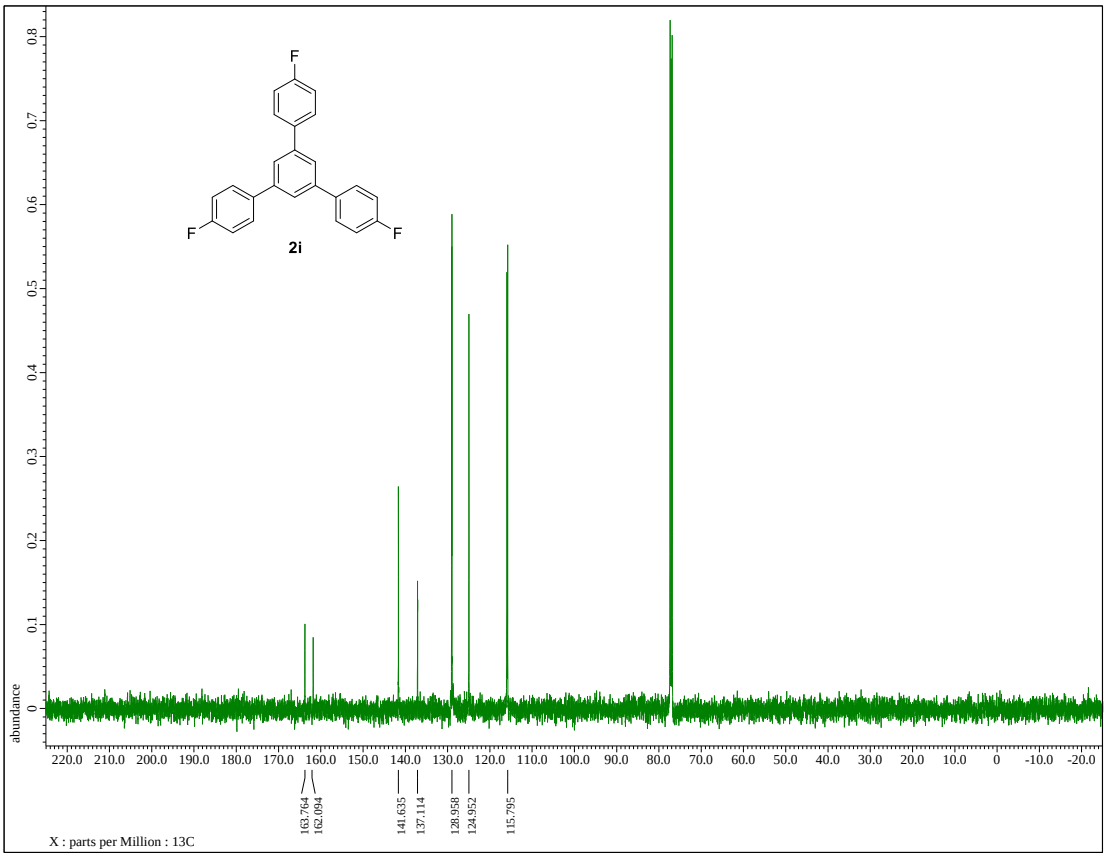

Figure S12-2. ^{13}C{^{1}H}-NMR spectrum of compound **2i** (125 MHz, $CDCl_3$)

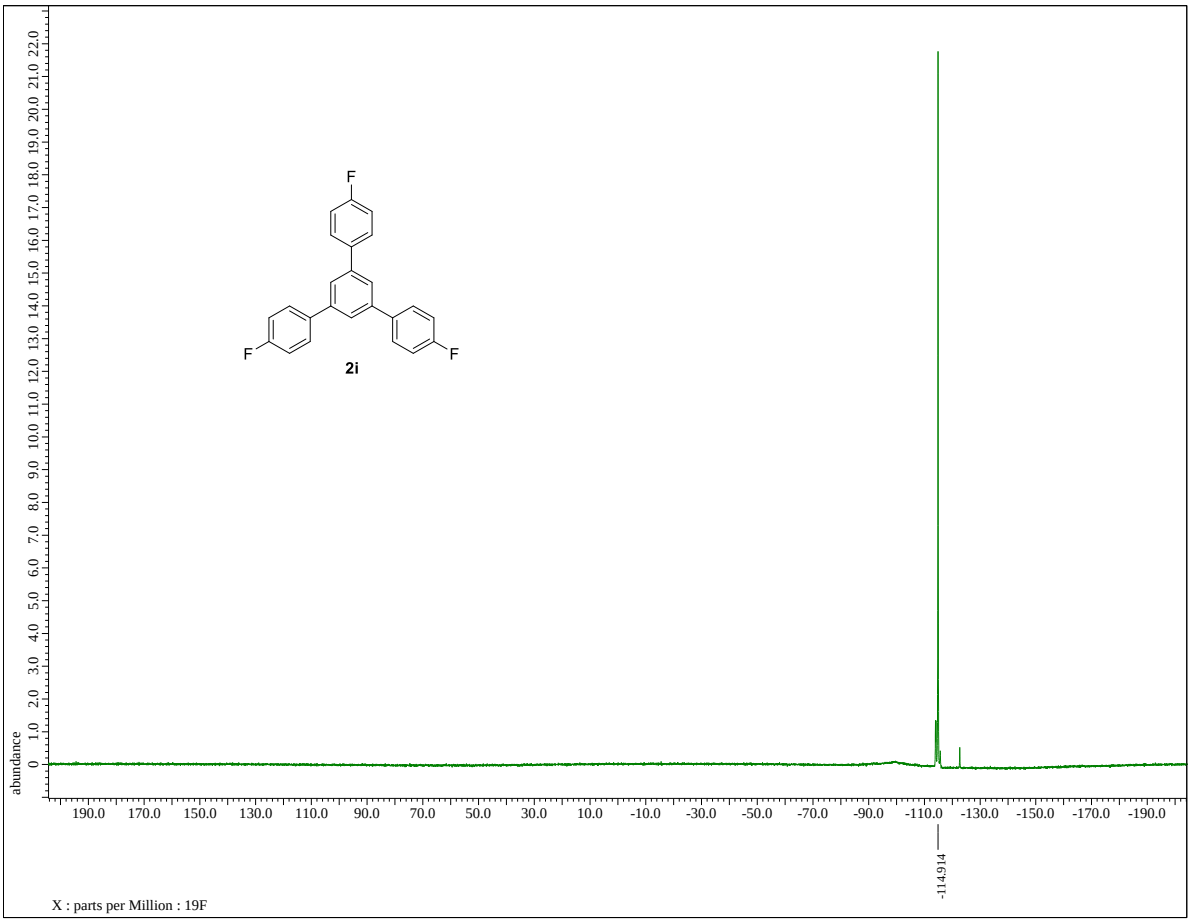

Figure S12-3. ^{19}F-NMR spectrum of compound **2i** (470 MHz, $CDCl_3$)

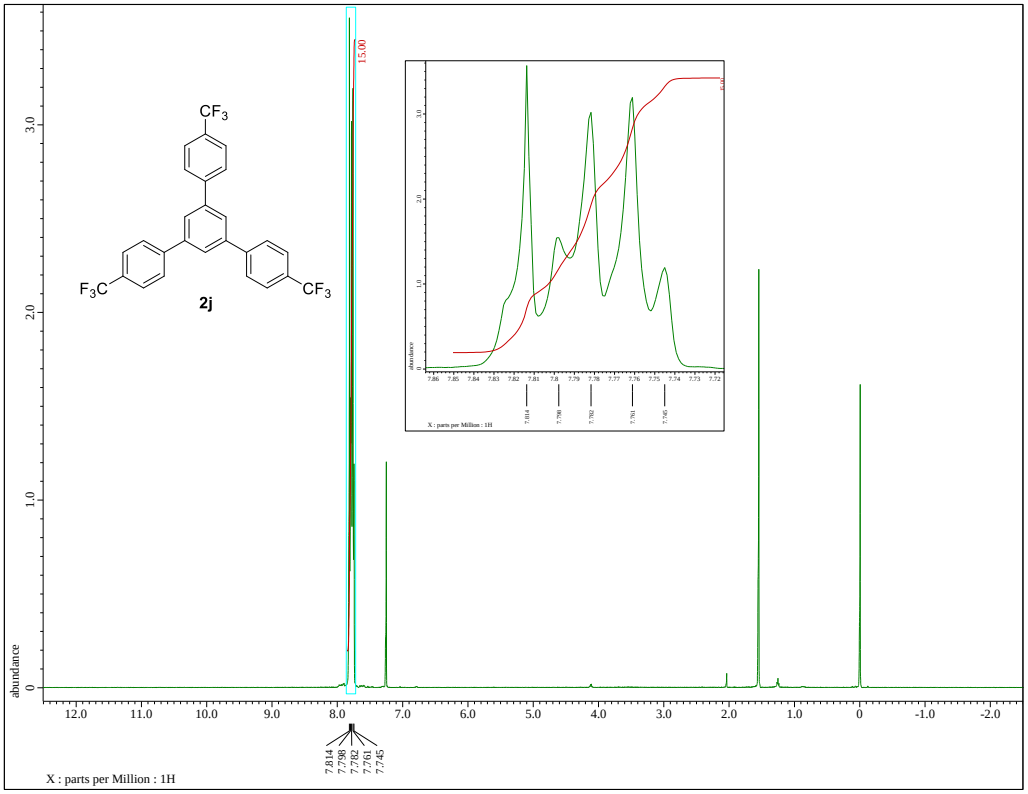

Figure S13-1. ^{1}H-NMR spectrum of compound **2j** (500 MHz, $CDCl_3$)

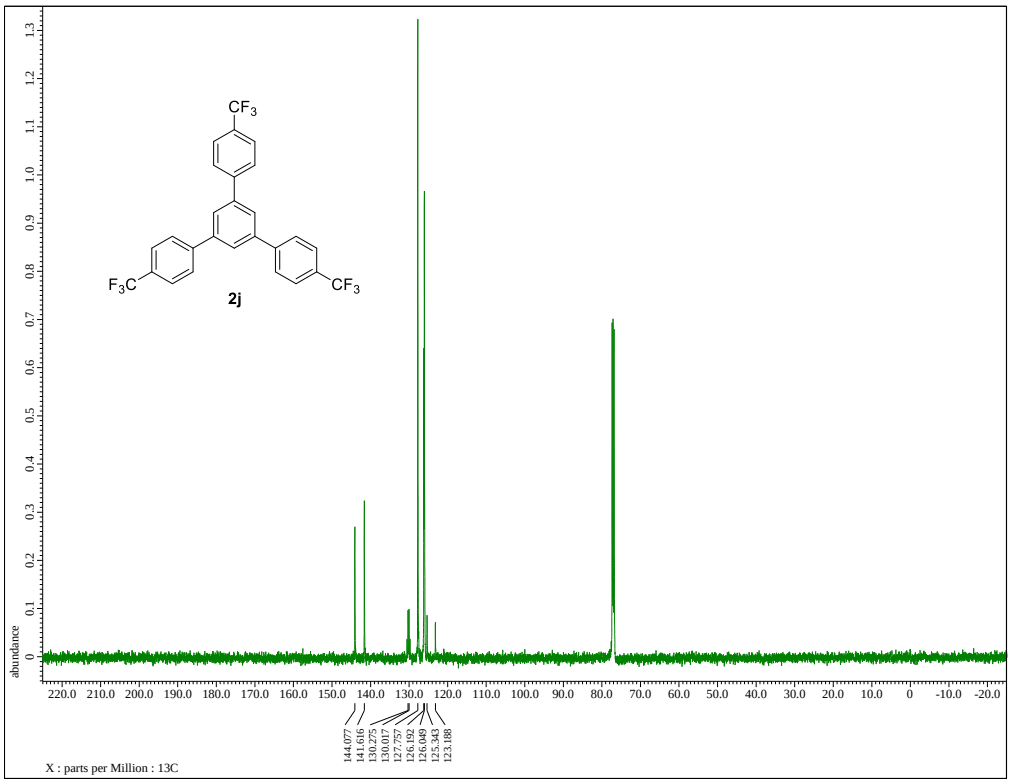

Figure S13-2. ^{13}C{^{1}H}-NMR spectrum of compound **2j** (125 MHz, $CDCl_3$)

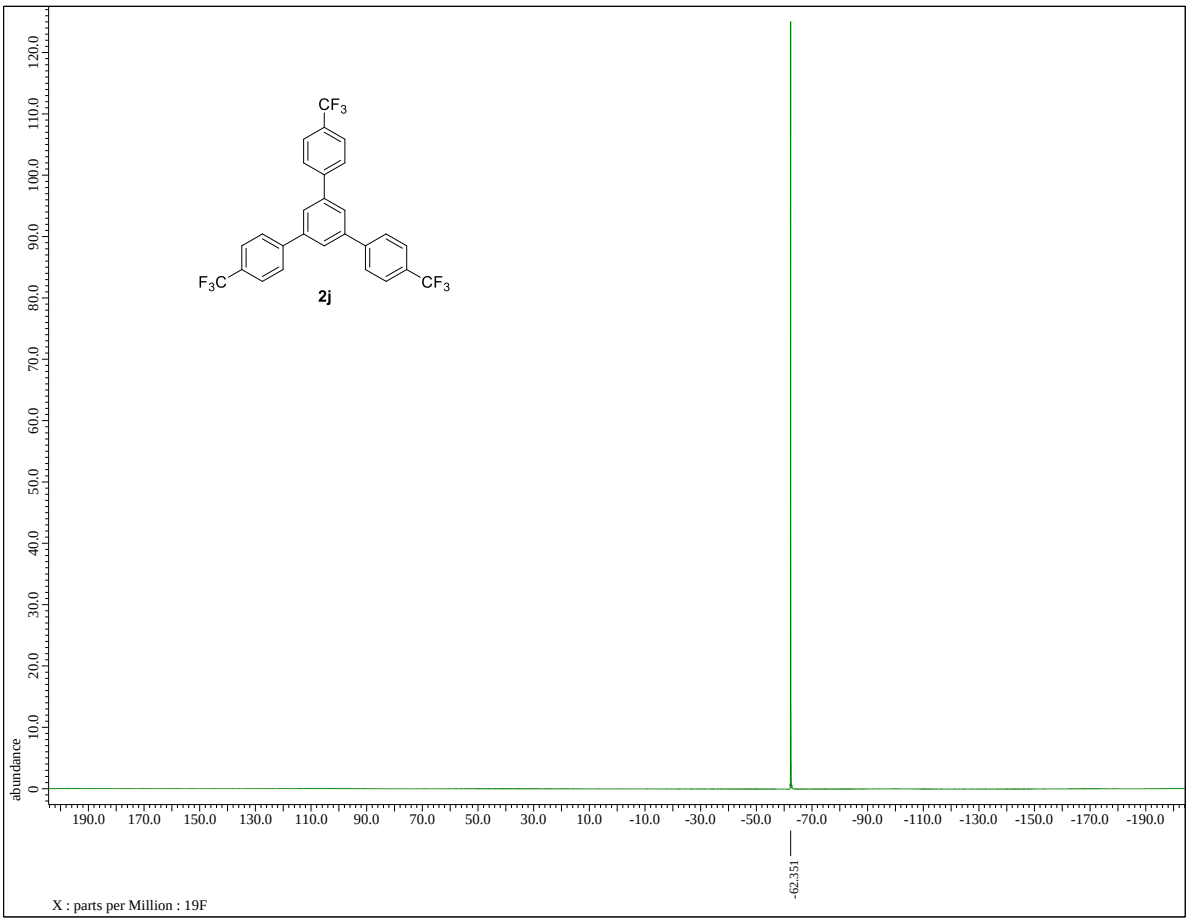

Figure S13-3. ^{19}F-NMR spectrum of compound **2j** (470 MHz, $CDCl_3$)

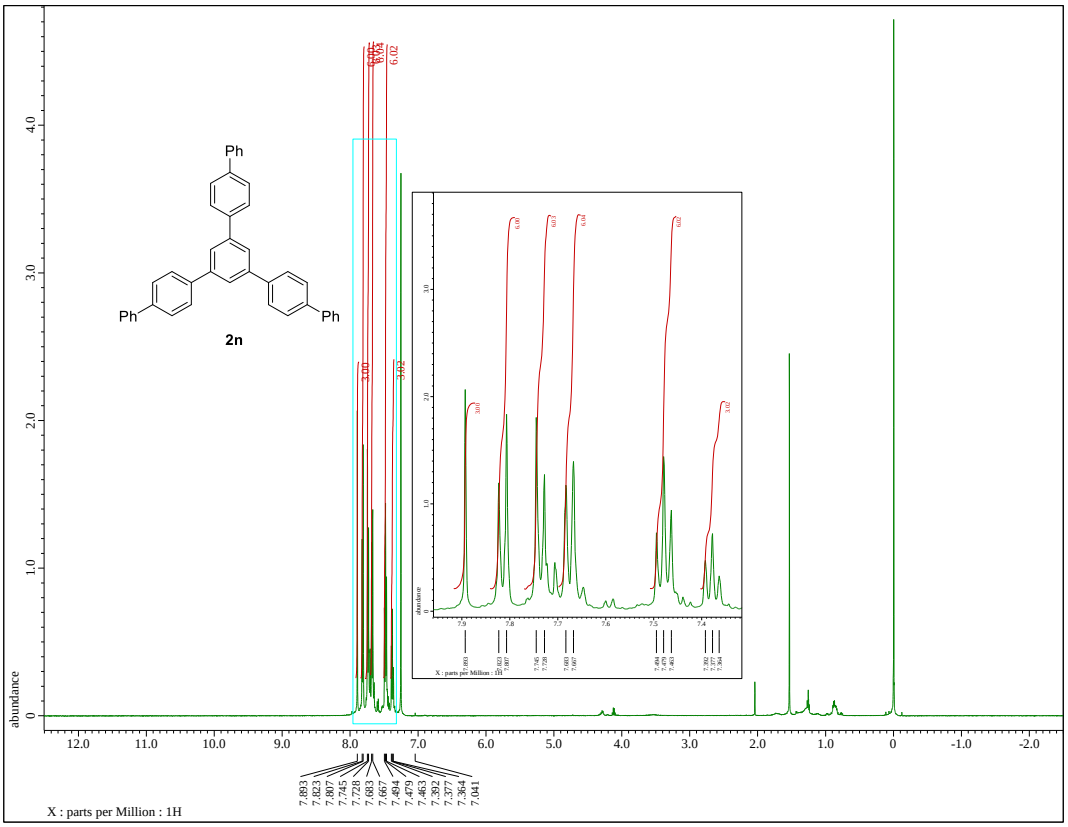

Figure S14-1. ^{1}H-NMR spectrum of compound **2n** (500 MHz, $CDCl_3$)

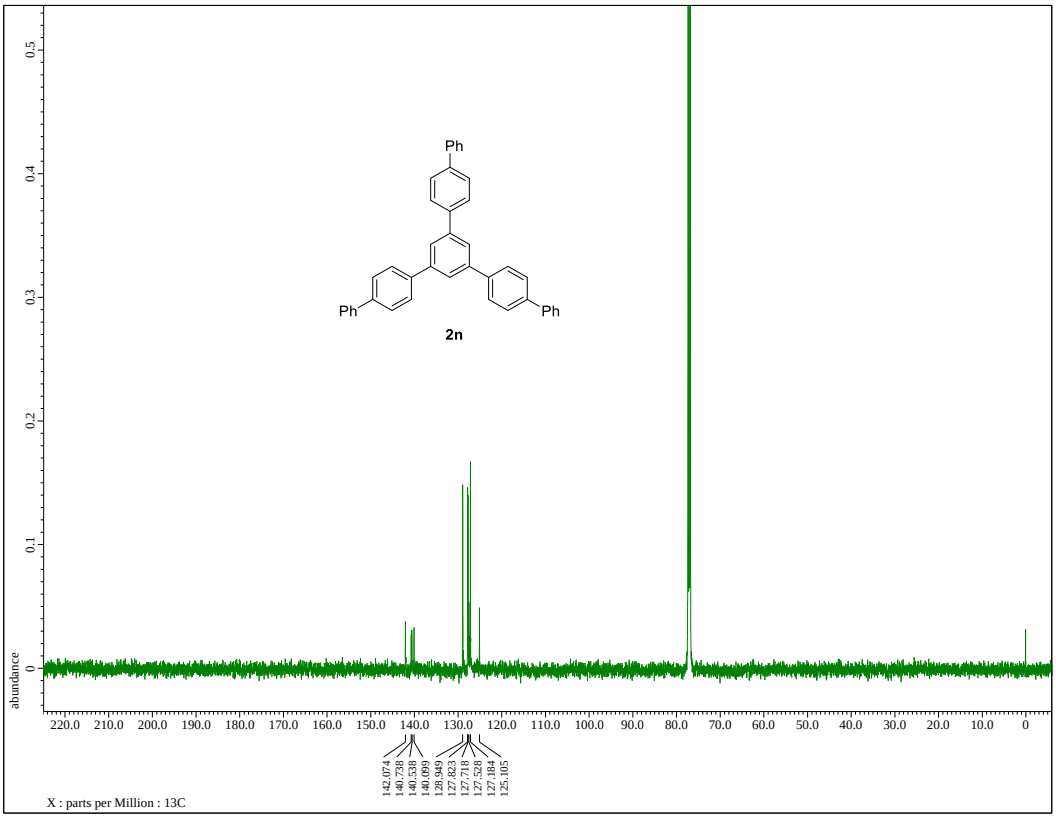

Figure S14-2. $^{13}C\{^{1}H\}$-NMR spectrum of compound **2n** (125 MHz, $CDCl_3$)

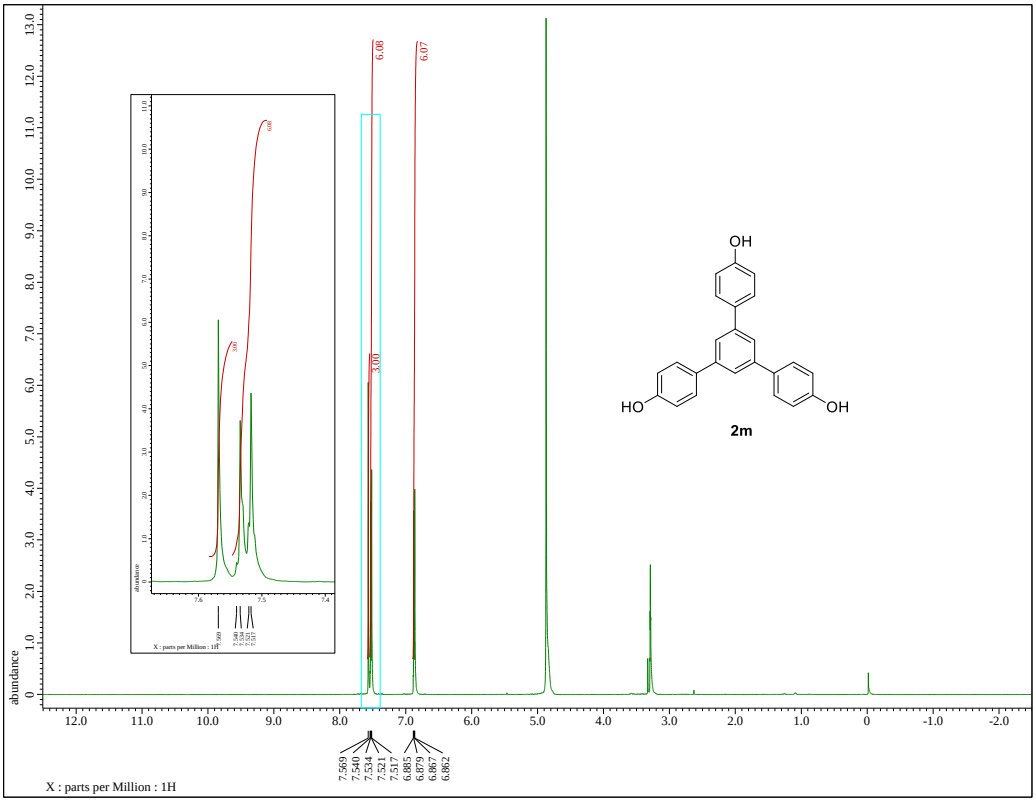

Figure S15-1. ^{1}H-NMR spectrum of compound **2m** (500 MHz, Methanol-d_3)

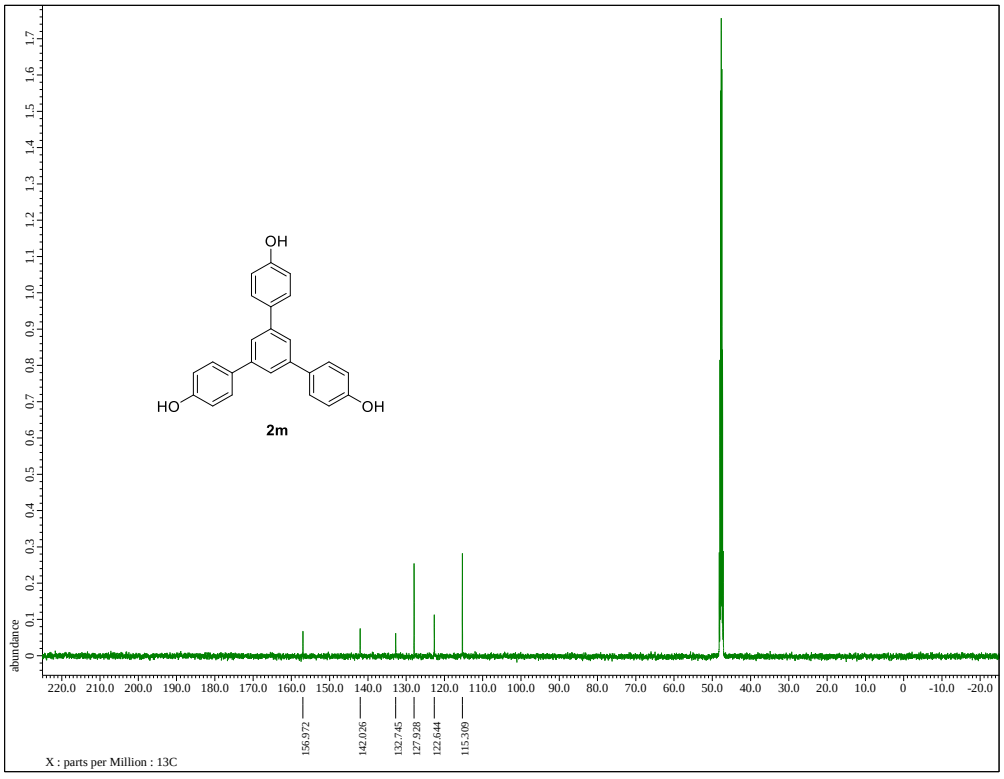

Figure S15-2. ^{13}C{^{1}H}-NMR spectrum of compound **2m** (125 MHz, Methanol-d_3)

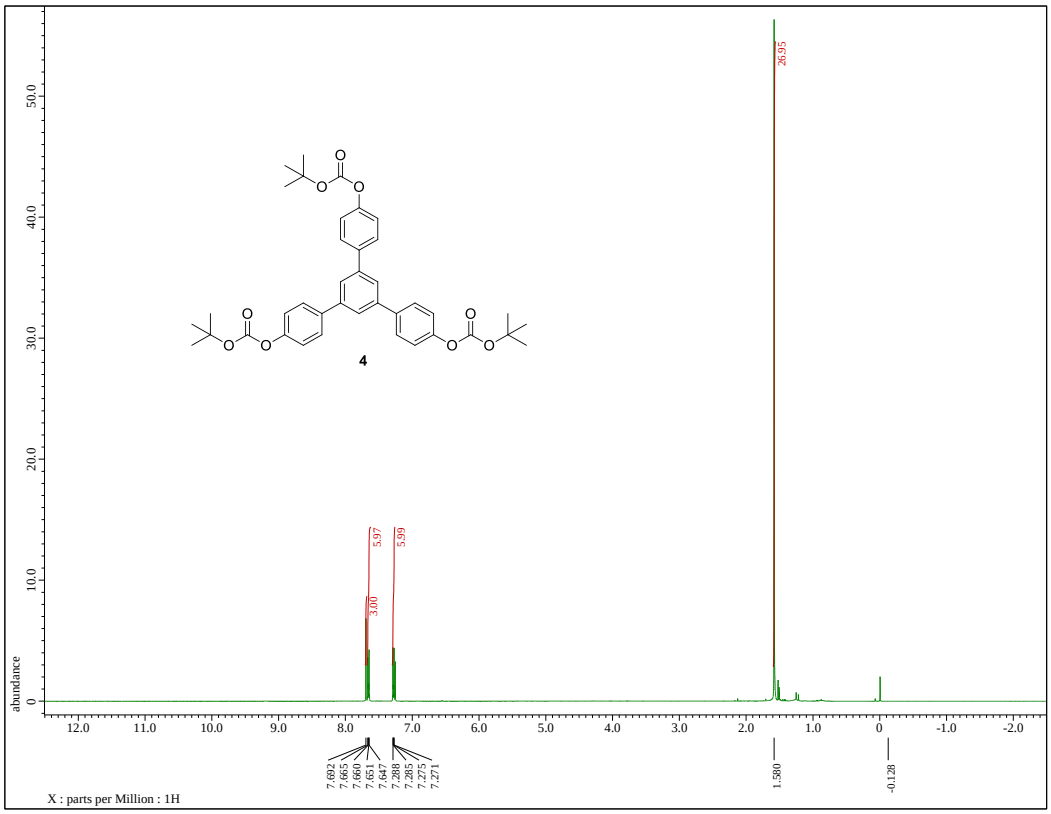

Figure S16-1. ^{1}H-NMR spectrum of compound **4** (500 MHz, $CDCl_3$)

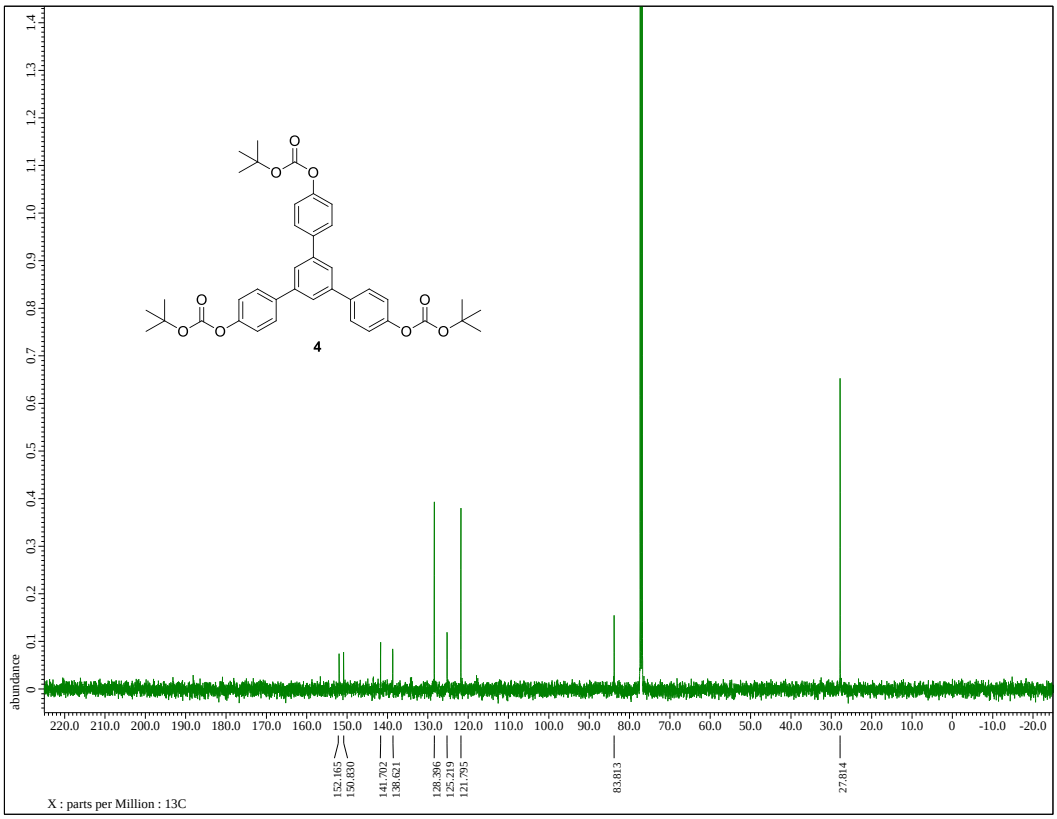

Figure S16-2. ^{13}C{^{1}H}-NMR spectrum of compound **4** (125 MHz, $CDCl_3$)

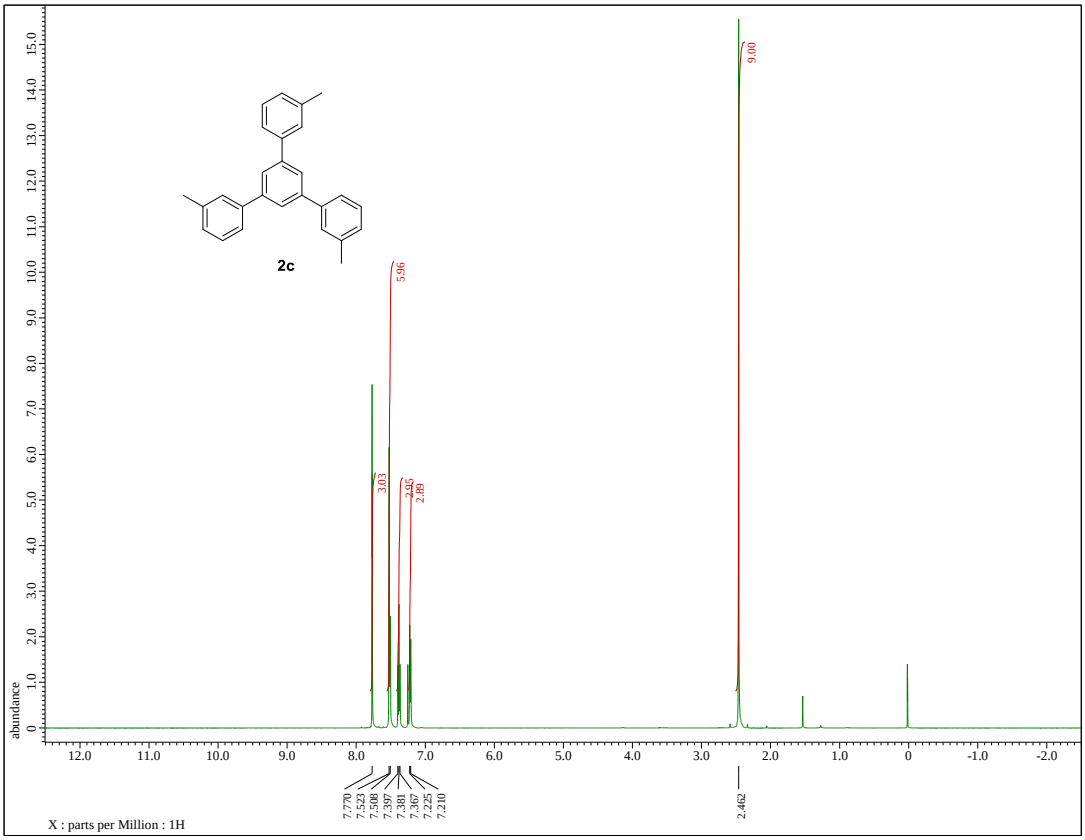

Figure S17-1. ^{1}H-NMR spectrum of compound **2c** (500 MHz, $CDCl_3$)

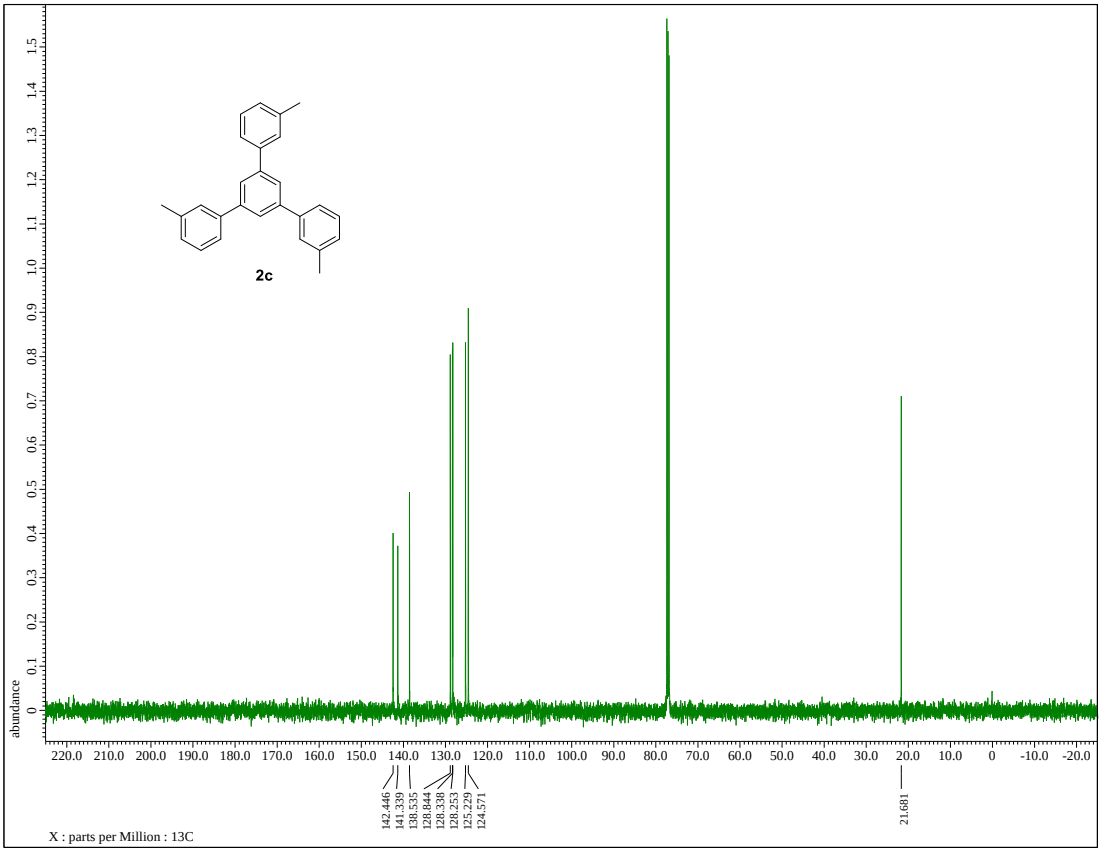

Figure S17-2. $^{13}C\{^{1}H\}$-NMR spectrum of compound **2c** (125 MHz, $CDCl_3$)

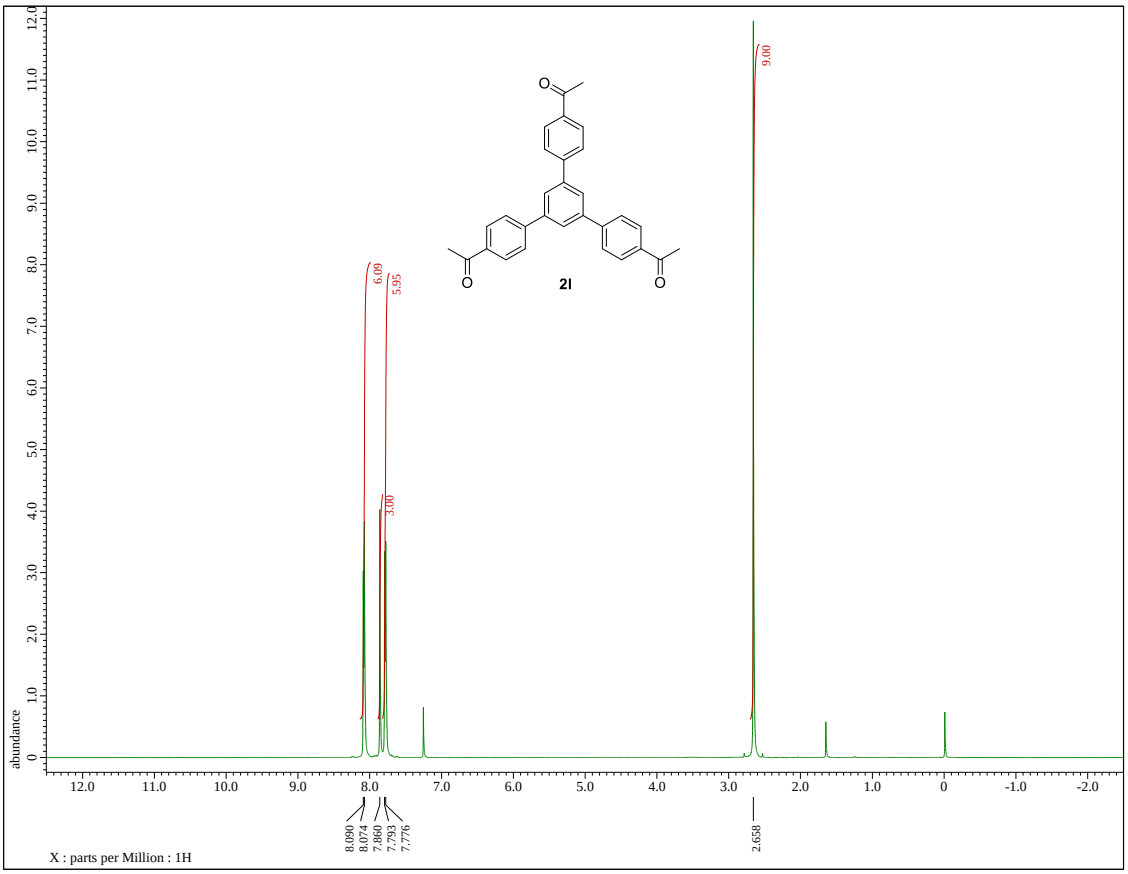

Figure S18-1. ^{1}H-NMR spectrum of compound **2l** (500 MHz, $CDCl_3$)

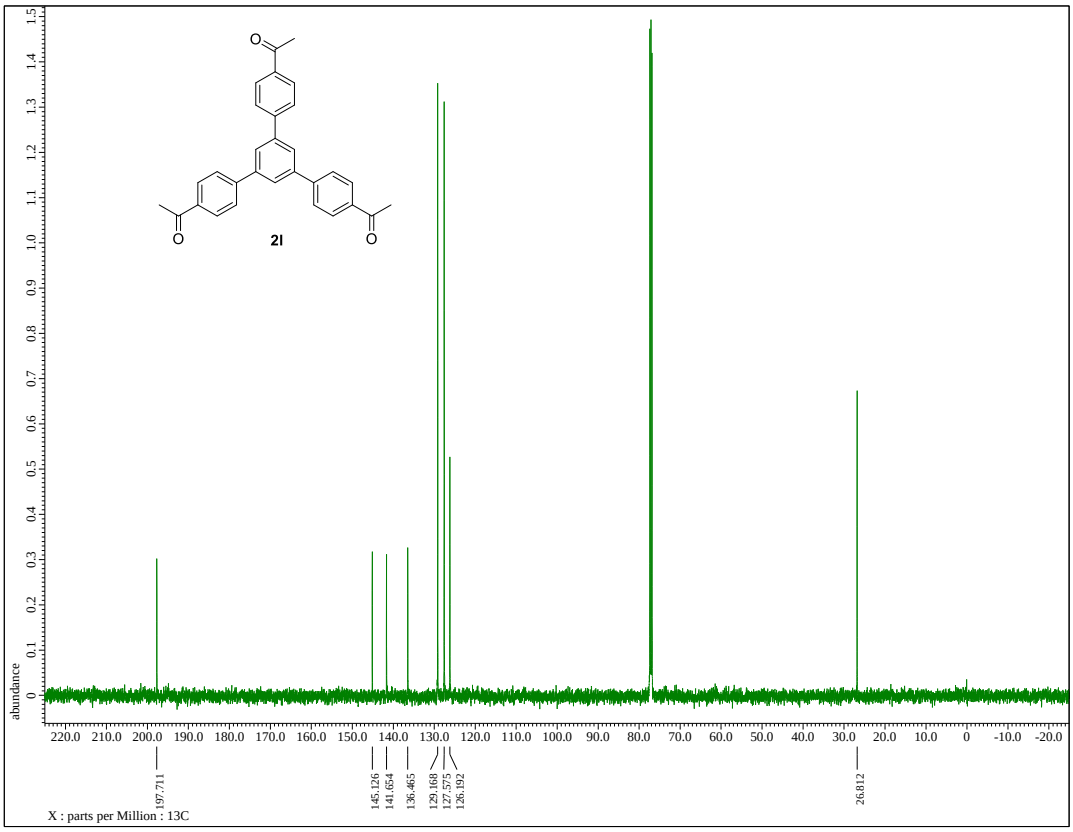

Figure S18-2. $^{13}C\{^{1}H\}$-NMR spectrum of compound **2l** (125 MHz, $CDCl_3$)

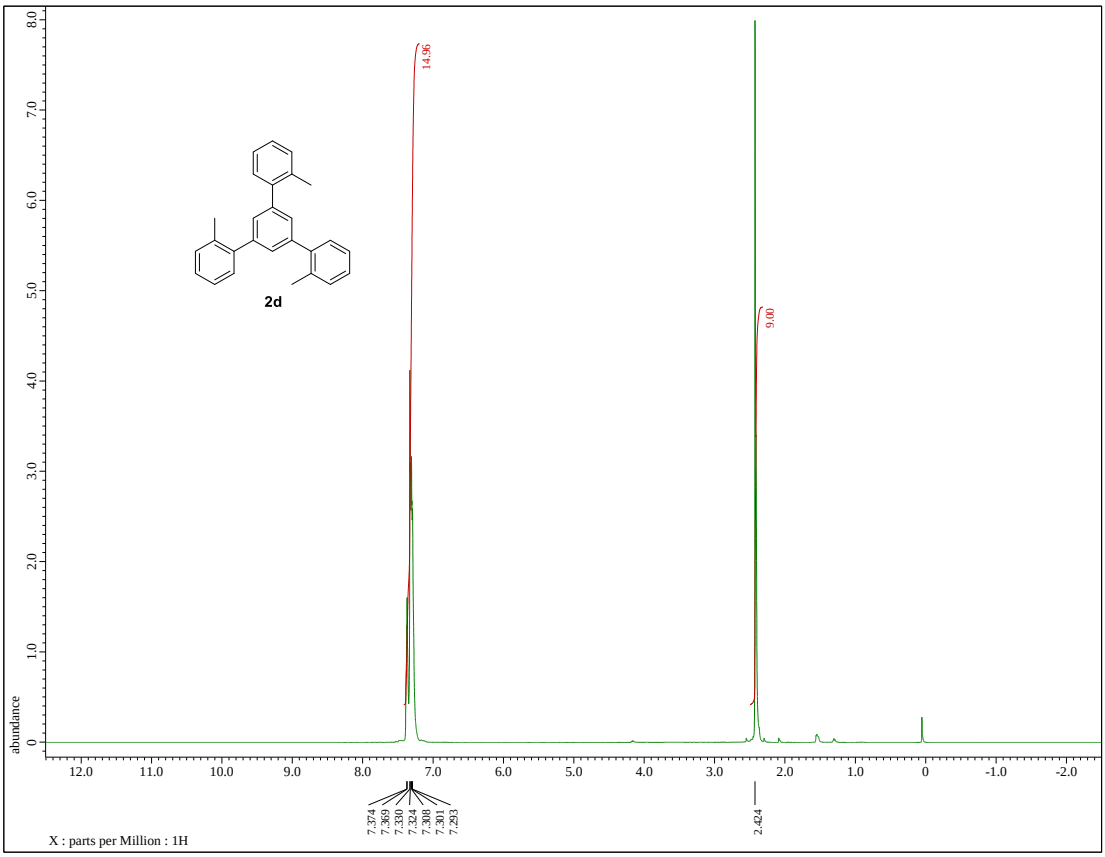

Figure S19-1. ^{1}H-NMR spectrum of compound **2d** (500 MHz, $CDCl_3$)

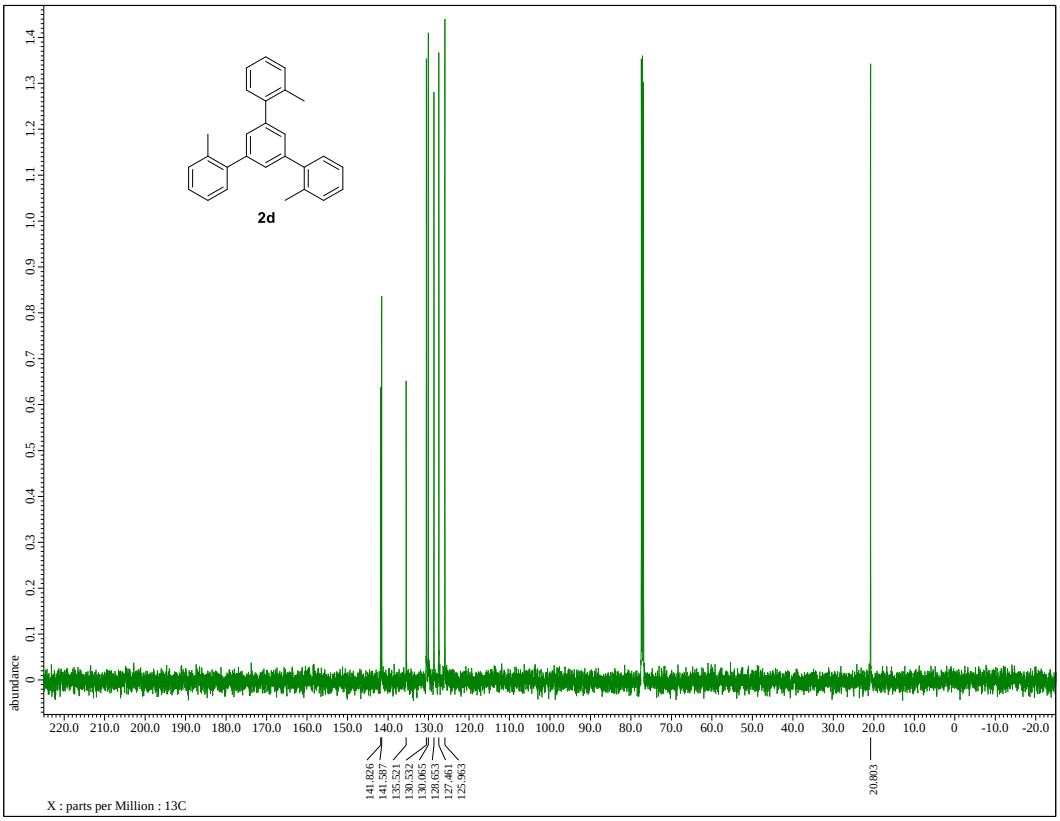

Figure S19-2. ^{13}C{^{1}H}-NMR spectrum of compound **2d** (125 MHz, $CDCl_3$)

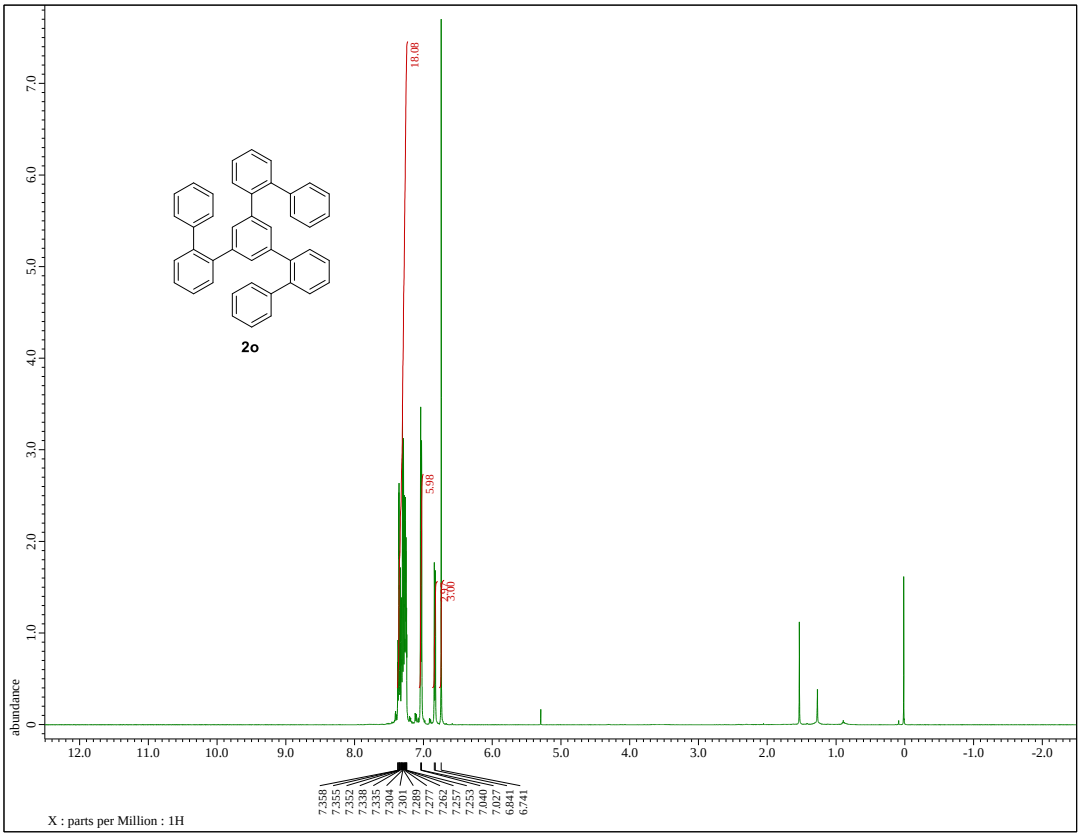

Figure S20-1. ^{1}H-NMR spectrum of compound **2o** (500 MHz, $CDCl_3$)

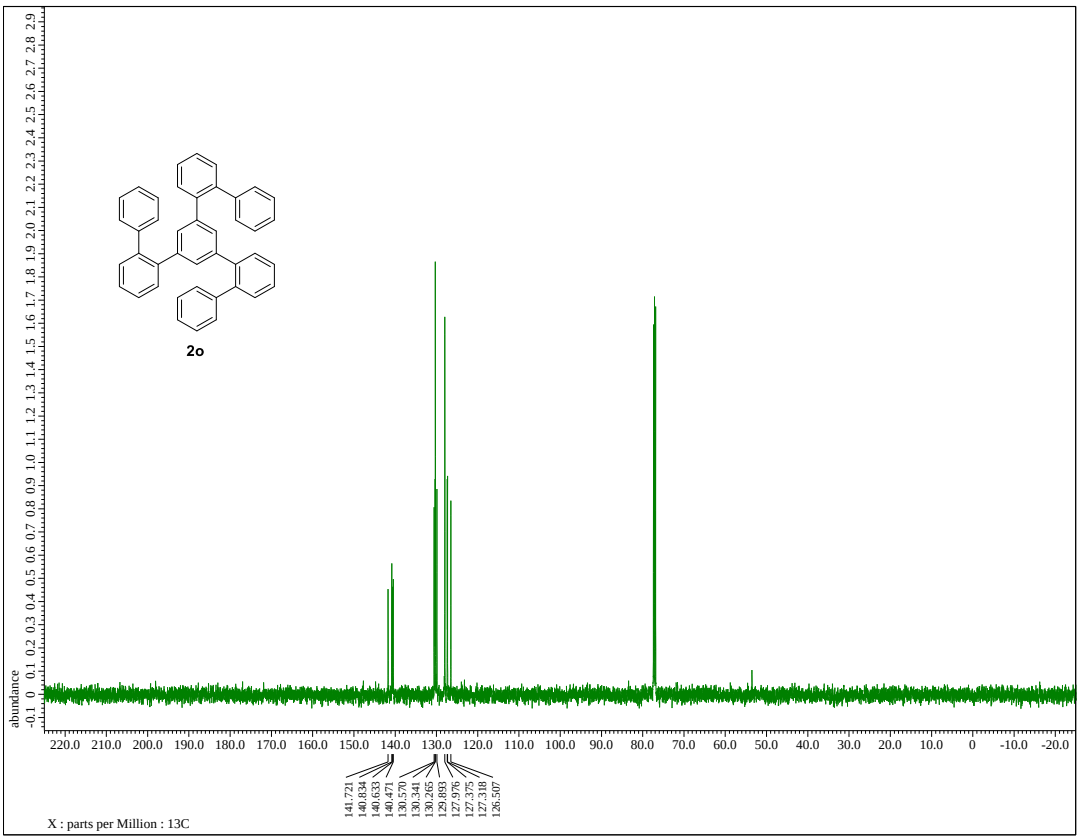

Figure S20-2. $^{13}C\{^{1}H\}$-NMR spectrum of compound **2o** (125 MHz, $CDCl_3$)

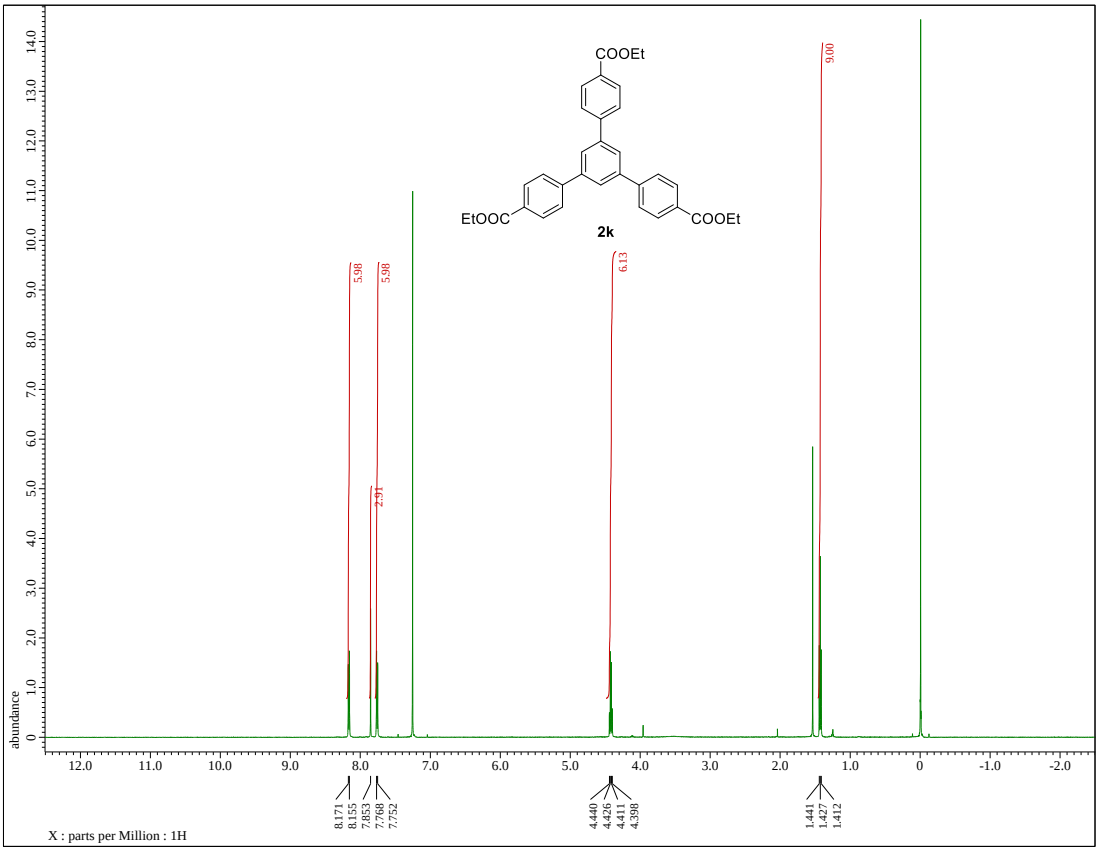

Figure S21-1. ^{1}H-NMR spectrum of compound **2k** (500 MHz, $CDCl_3$)

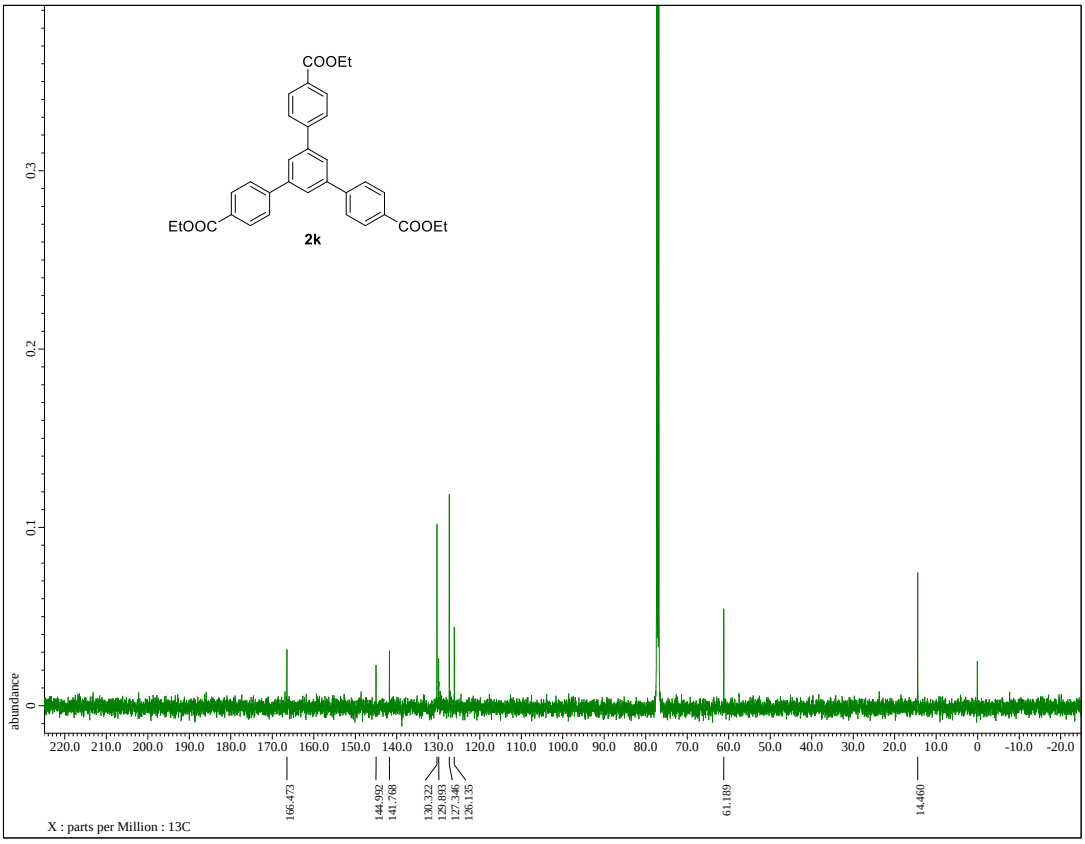

Figure S21-2. ^{13}C{^{1}H}-NMR spectrum of compound **2k** (125 MHz, $CDCl_3$)

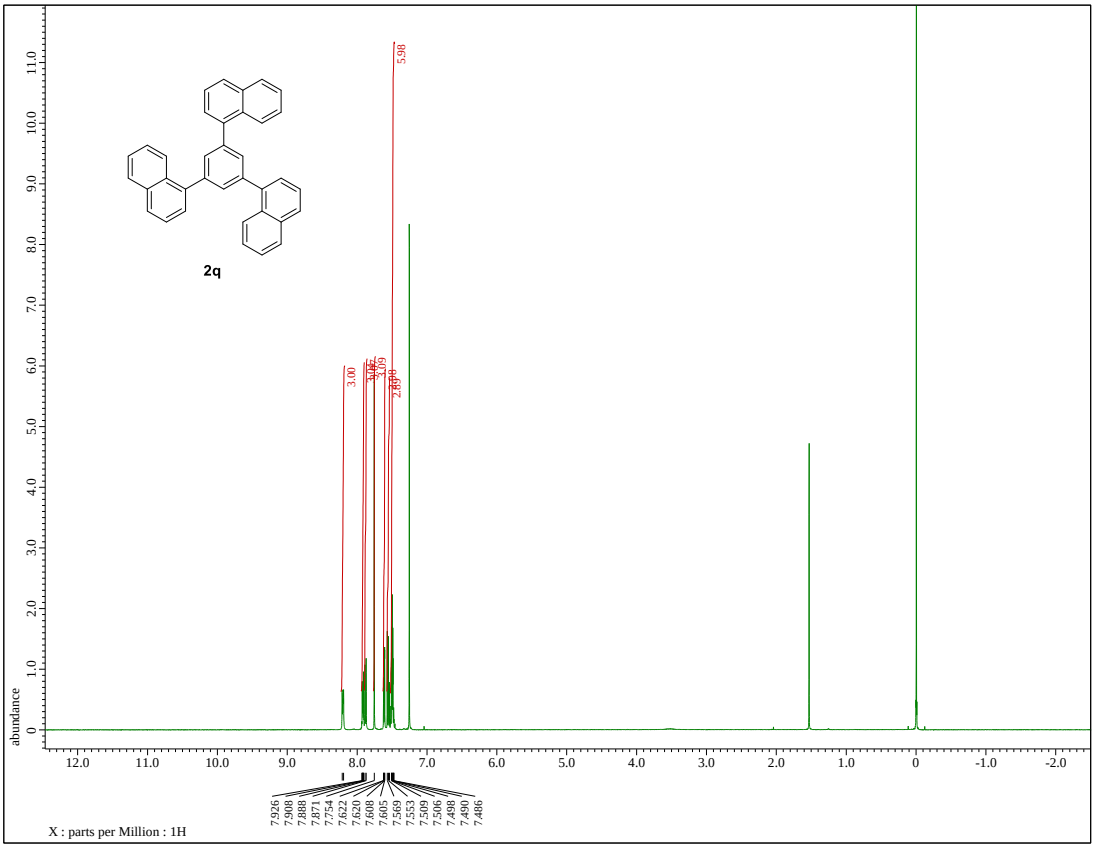

Figure S22-1. ^{1}H-NMR spectrum of compound **2q** (500 MHz, $CDCl_3$)

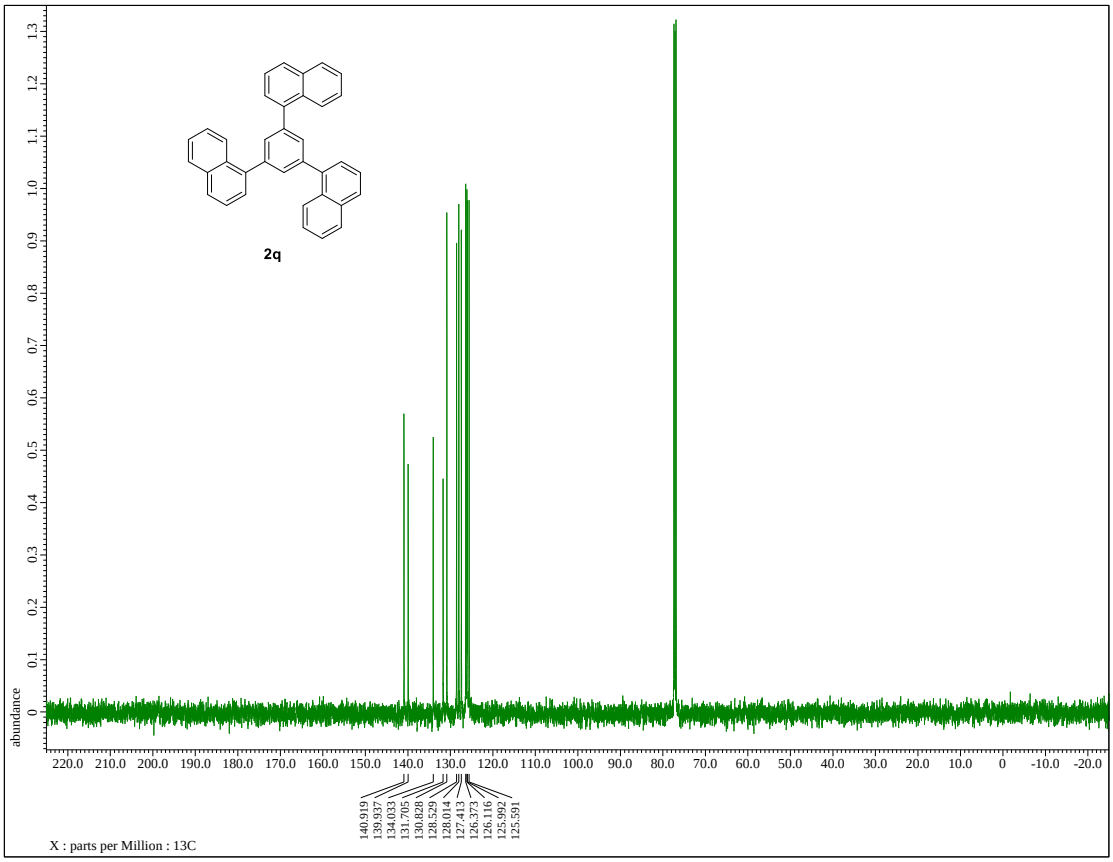

Figure S22-2. $^{13}C\{^{1}H\}$-NMR spectrum of compound **2q** (125 MHz, $CDCl_3$)

18. MALDI-TOF-MS data:

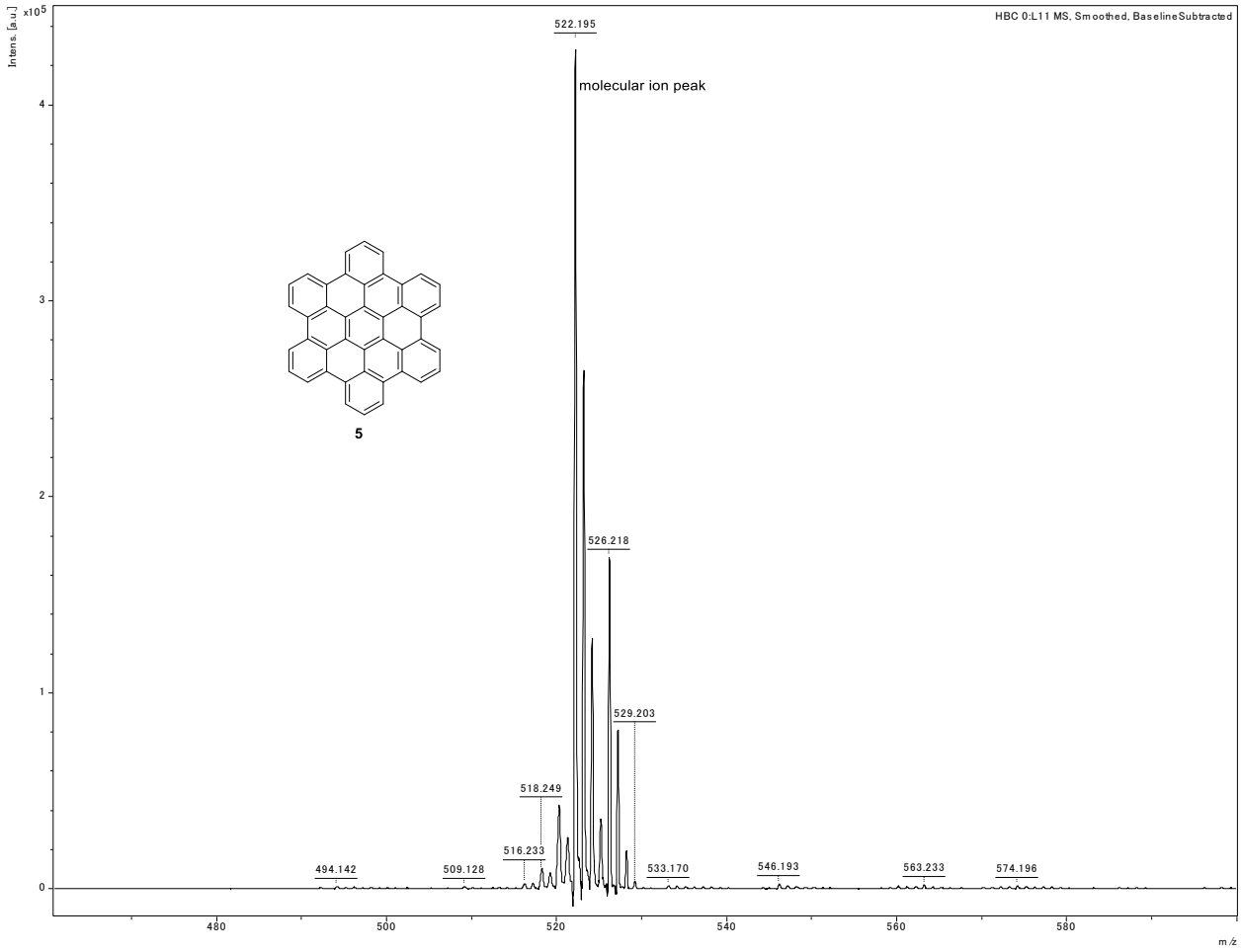

Figure S23. MALDI-TOF MS of Compound **5** (Matrix: 2,5-dihydroxybenzoic acid)

19. Crude GC-MS Analysis

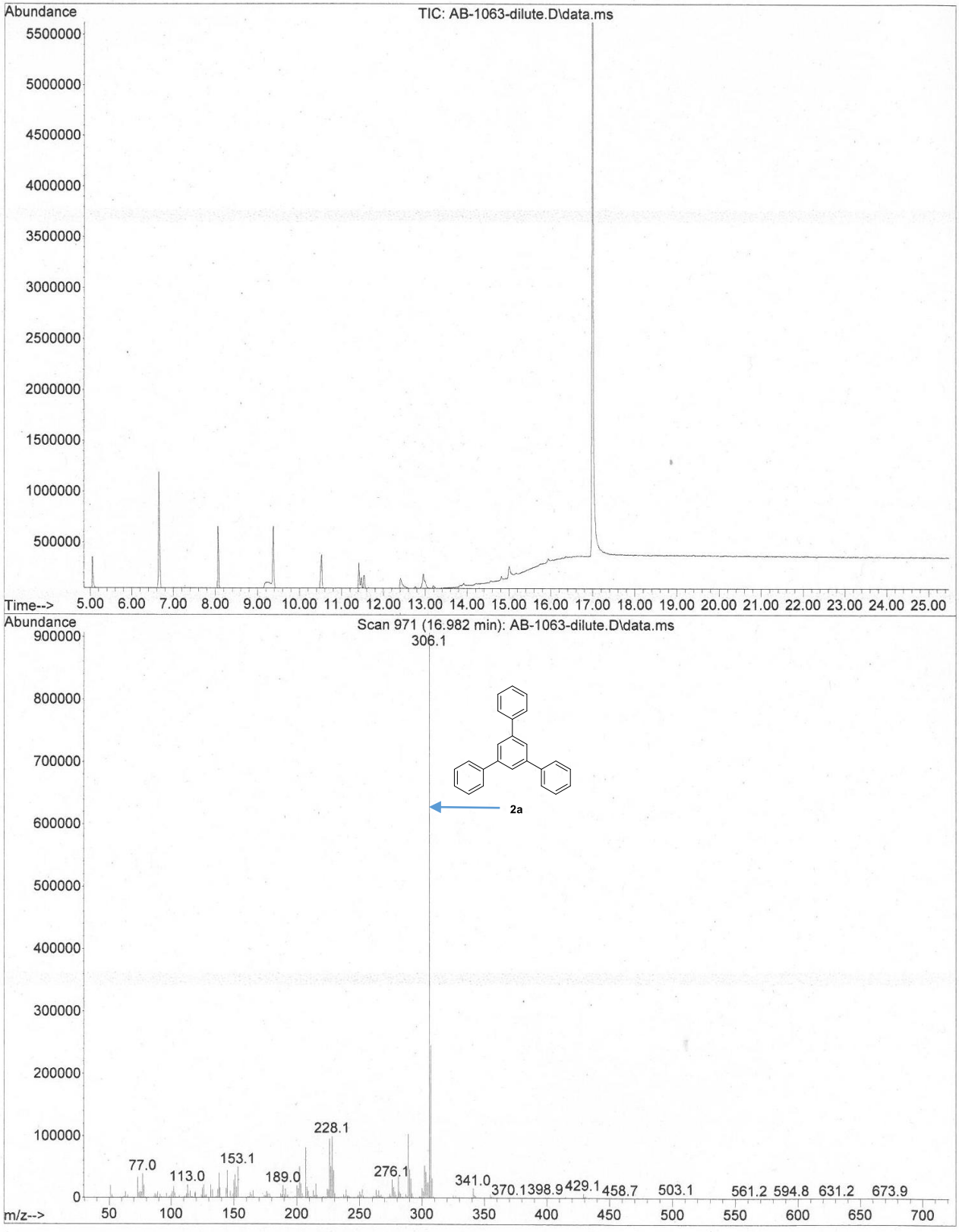

Figure S24-1. GC-MS analysis of crude reaction mixture (overall)

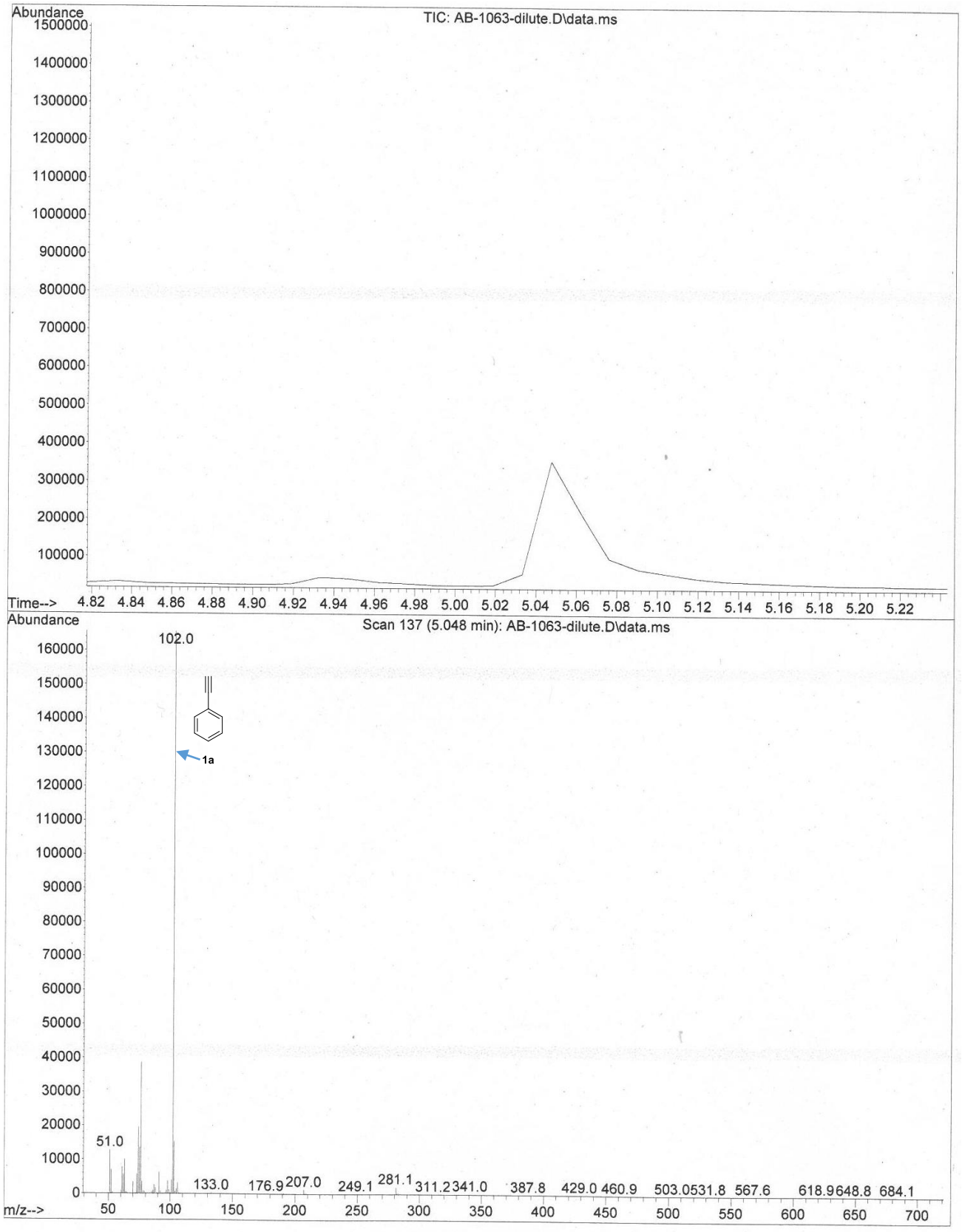

Figure S24-2. GC-MS analysis of crude reaction mixture (enlarged view for **1a**)

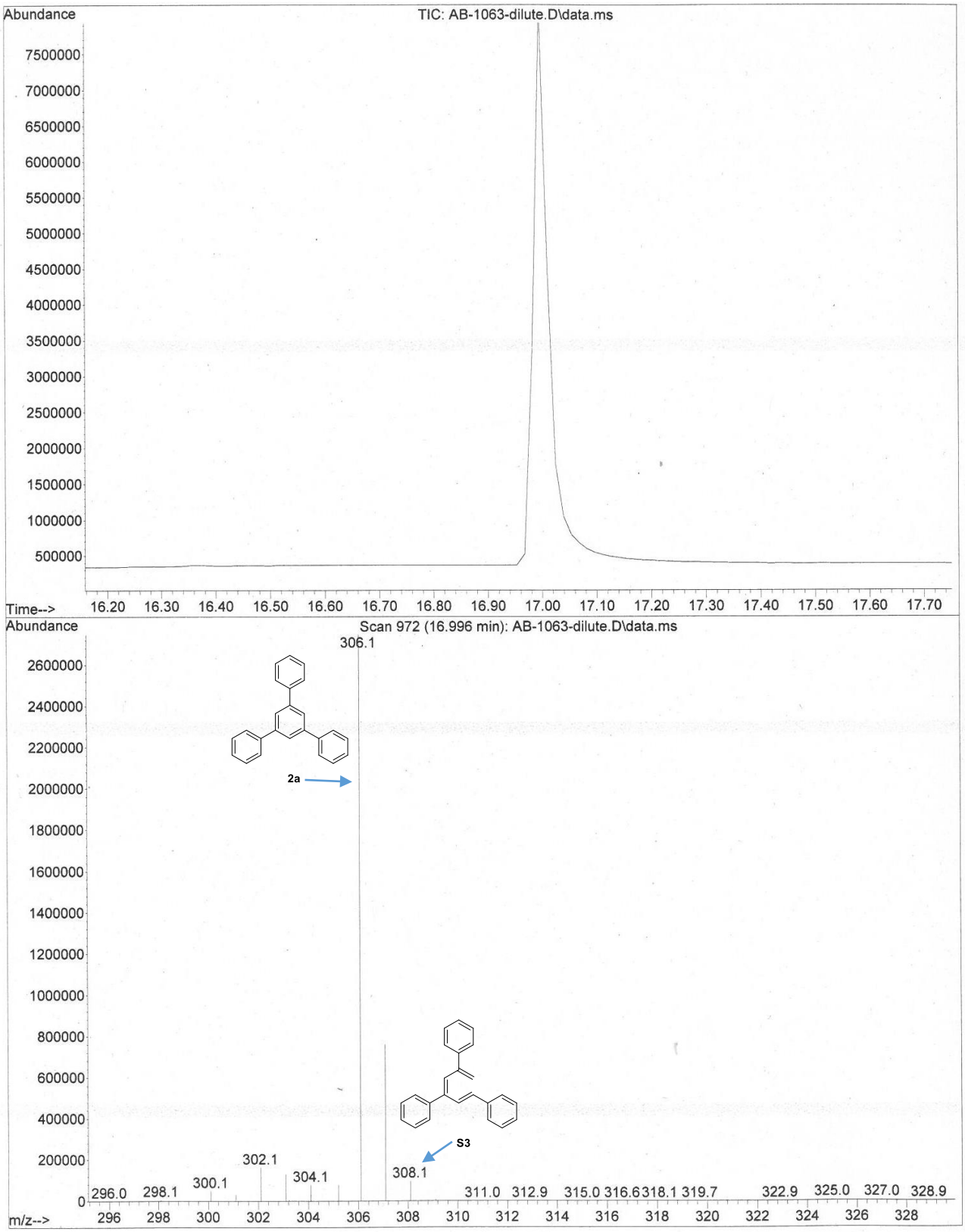

Figure S24-3. GC-MS analysis of crude reaction mixture (enlarged view for **2a** and **S3**)

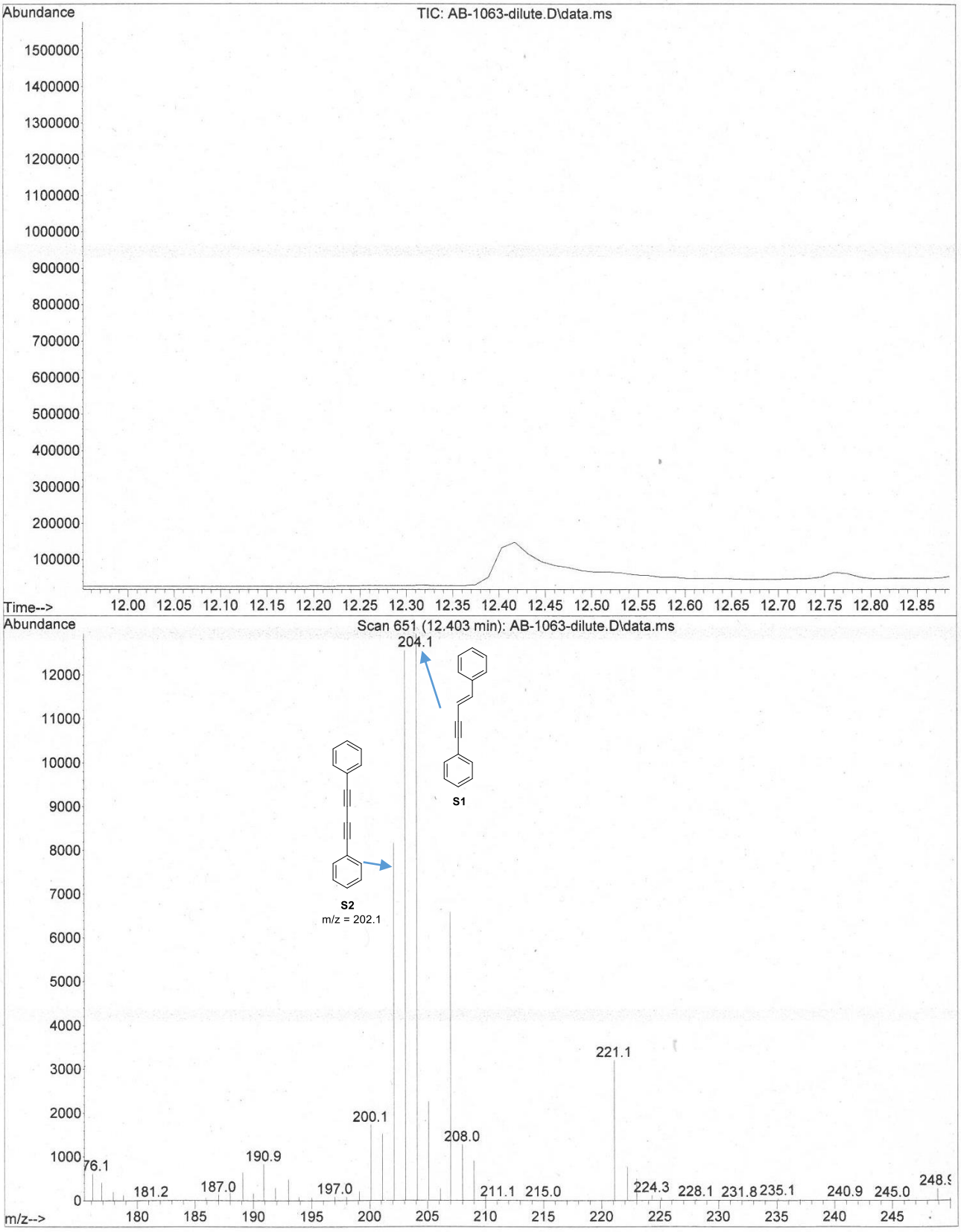

Figure S24-4. GC-MS analysis of crude reaction mixture (enlarged view for **S1** and **S2**)